Available online at www.sciencedirect.com
SCIENCE DIRECT®
Coordination Chemistry Reviews 243 (2003) 237–262
COORDINATION CHEMISTRY REVIEWS
www.elsevier.com/locate/ccr

The stereochemistry of the copper(II) ion in the solid-state—some recent perspectives linking the Jahn–Teller effect, vibronic coupling, structure correlation analysis, structural pathways and comparative X-ray crystallography

Brian Murphy [a,*], Brian Hathaway [b,1]

[a] *Department of Chemistry, United Arab Emirates University, P.O. Box 17551, Al-Ain, United Arab Emirates*
[b] *Department of Chemistry, University College Cork, Cork, Ireland*

Received 26 June 2001; accepted 23 April 2003

Contents

Abstract

It is now over 60 years since the Jahn–Teller theorem was put forward and shown to account for the distorted stereochemistry of copper(II) complexes. Numerous accounts have been written describing the origin of the distortion. However, recent work, involving the emerging field in structural chemistry of comparative X-ray crystallography, has shown that the vibronic coupling mechanism can now be applied to low symmetry systems, suggesting that the original static stereochemistries are all connected and continuously variable. This review of copper(II) stereochemistry involving structural pathways is presented here in an attempt to describe and rationalise these variable stereochemistries. Some recent perspectives and new interpretations linking the Jahn–Teller effect (JTE), vibronic coupling, structure correlation analysis, structural pathways and comparative X-ray crystallography are reported.

Keywords: Copper(II) stereochemistry; Jahn–Teller; Vibronic coupling; Structure correlation analysis; Structural pathways; Comparative X-ray crystallography

* Corresponding author.
E-mail address: murphy.brian@uaeu.ac.ae (B. Murphy).
[1] Deceased.

0010-8545/03/$ - see front matter © 2003 Elsevier Science B.V. All rights reserved.
doi:10.1016/S0010-8545(03)00084-5

1. Introduction

Sixty-six years ago in 1937, Jahn and Teller published the first approximate formulation of the Jahn–Teller effect (JTE) [1] and stated that the nuclear configuration of any non-linear polyatomic system in a degenerate electronic state is unstable with respect to nuclear displacements, that lower the symmetry, and remove the degeneracy. Numerous accounts have been written on the JTE and how it plays a pivotal role in the range of distorted stereochemistries of octahedral copper(II) complexes. In a recent (2001) in-depth and comprehensive review [2] on modern aspects of the JTE Theory and its applications to molecular problems, Bersuker shows how in a more thorough approach the JTE can be separated from the JT theorem. Bersuker states that the JT theorem refers to the adiabatic potential energy system (APES), which, although not seen directly, can give an indirect qualitative measure of many observable effects. The JT theorem states that if the APES of a polyatomic system has two or more branches that intersect in one point (the degeneracy point Q_0), then at least one of them has no extremum at this point. Two types of cases are exceptions: (a) linear molecules (linear configurations at Q_0); and (b) twofold spin (Kramers) electronic degeneracy. An appropriate proof of the theorem is described in the review and references therein.

Overall, the JTE itself continues to be an area of prolific research in coordination chemistry and recently has been shown to play an important role in high-T_c cuprate superconductors [3] and in colossal magnetoresistance [4], involving a massive increase in the size of magnetoresistance seen in devices such as magnetic tape and disk readers, linked to the Jahn–Teller active manganese(II) centre. In the case of the cuprate superconductors, a number of models have been proposed describing the role of JT-active centres in such systems [5–7].

2. Types of Jahn–Teller (JT) systems

2.1. The classic $E \otimes e$ vibronic coupling JT problem (copper(II) complex without strain)

Quality theoretical descriptions of JT systems [2,8,9] are critical in providing information not only on the energy levels but also on the vibronic states that then can be employed in the modelling of specific systems in order to interpret experimental data. In the specific case of copper(II) stereochemistry, numerous accounts have been written describing the origin of the distortion of an octahedral CuL_6 chromophore to an elongated tetragonal or rhombic octahedral stereochemistry (EO).

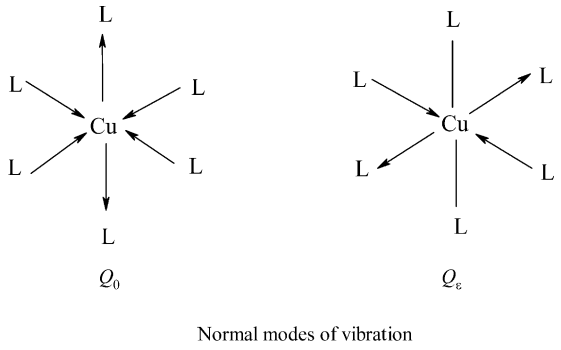

Fig. 1. The forms of distortion of an octahedral CuL_6 chromophore.

Several detailed reviews can be found in the literature [10–16] by Bersuker, Hathaway, Falvello, Hitchman, Simmons and other authors describing the JT effects in solid-state coordination chemistry. However, the cubic JT system that has warranted the most attention to date is the $E \otimes e$ JT system [9]. The form of the distortion can be any of the non-totally symmetric normal modes of vibration of the CuL_6 chromophore. In the O_h point group, the direct product $e_g \otimes e_g$ reduces to $a_{1g} \oplus a_{2g} \oplus e_g$. However, a_{1g} is totally symmetric, a_{2g} is not present, and e_g represented by the components, Q_ε and Q_θ (Fig. 1), is the only active JT mode [13,17]. The distortion then originates in the doubly degenerate ^2E_g ground state of the d^9 configuration, $t_{2g}^6 e_g^3$, by coupling of the electronic energy with the e_g modes of vibration of the regular octahedral CuL_6 chromophore, involving the Q_ε and Q_θ modes of Fig. 1 to remove the degeneracy. The energy surface arising from this coupling, derived from a

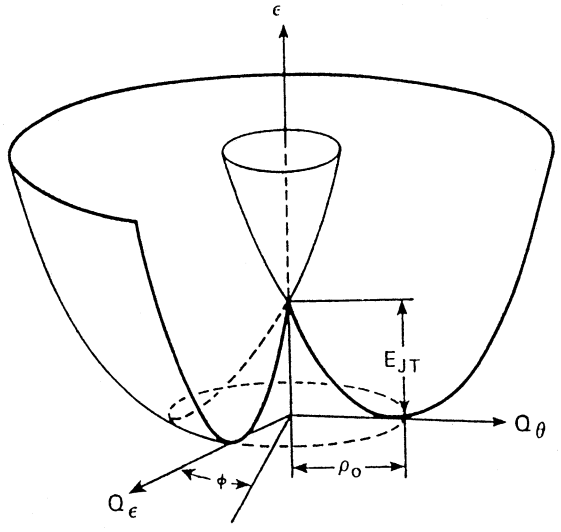

Fig. 2. *Mexican Hat* Model for the linear $E \otimes e$ problem. This is the APES for a twofold degenerate E term which interacts linearly with the twofold degenerate E-type vibrations, shown by the Q_θ and Q_ε coordinates. There is a conical intersection at $Q_\theta = Q_\varepsilon = 0$. The JT stabilisation energy is given by E_{JT} and the radius of the trough is given by ρ_0. (Reprinted with permission from Ref. [17]. Copyright 1996 John Wiley & Sons, Inc.)

perturbation theory, taken to second order, has been described in detail in the literature and this model is termed the '*Mexican Hat*' model (Fig. 2) [2,17,18]. Bersuker has reviewed comprehensively [2] this most classic and simplest of JT problems and has described how the linear and quadratic coupling terms of the vibronic interaction, W, expressed by the equation:

$$W(r,\ Q) = V(r,\ Q) - V(r,\ 0) = \sum\nolimits_{\alpha} (\partial V/\partial Q_{\alpha})Q_{\alpha} + \frac{1}{2}\sum\nolimits_{\alpha,\beta} (\partial^2 V/\partial Q_{\alpha}\partial Q_{\beta})_0 Q_{\alpha}Q_{\beta} + \cdots$$

given by independent constants, imply that the quadratic coupling is not minor when compared to the linear coupling. If the quadratic coupling is large, the APES changes and its associated properties. Bersuker also has referred in his review how the general consensus from theoretical work in this area that the ground vibronic state has the same degeneracy and symmetry E as the initial electronic state (at the point of degeneracy) should in fact be reversed. In a related paper [17], Bersuker has shown by direct numerical calculations that, if g, the quadratic coupling is sufficiently large, the first excited non-degenerate vibronic energy level A, intersects with the lower, ground level, E, and remains the ground state for bigger g values. The net effect then is that if g is large enough, the three conical intersections move towards the central conical intersection, generating a substitute route for tunnelling between near-neighbour minima. Such a route encompasses all four conical intersections as opposed to that for values of small g, which only encompass the one central conical intersection.

An understanding of this classic $E \otimes e$ JTE is important as it can be used to validate concepts before applying it globally to more complex systems. This $E \otimes e$ vibronic coupling can be applied to copper(II) systems where there are six chemically equivalent ligand atoms, with cubic or trigonal crystallographic site symmetries.

2.2. The dynamic JTE

In general, the hopping of a distortion from one orientation to another is termed the dynamic JTE [13,16,19]. In the '*Mexican Hat*' model, if the barrier height between minima is less than kT, all three minima will be populated equally [13]. The complex in question [20–22] will then show trigonal or octahedral symmetry, as a result of a dynamic interconversion of the three equivalent elongated tetragonal distortions of the nuclear framework. In the dynamic JT process, the following interchanges can be involved:

i) A three-dimensional dynamic interchange between three mutually perpendicular directions of the distortion to yield a *pseudo octahedral* stereochemistry;
ii) A two-dimensional dynamic interchange to yield a *pseudo compressed octahedral* stereochemistry or;
iii) A more limited one-dimensional distortion, which only displays *limited* variability with temperature, termed *fluxional* behaviour, and which ultimately yields a *static elongated* or *rhombic octahedral* stereochemistry.

In all three situations, the strict operation of the JTE only applies to regular CuL_6 chromophores with six equivalent ligands, and examples of such complexes are surprisingly limited, considering the breadth of complexes of known crystal structure known to 2003 in copper(II) stereochemistry. Fig. 3 summarises the stereochemistries of the copper(II) ion, their approximate point group symmetries and their occurrence in 1970. Table 1 gives examples of complexes of different stereochemistries of the copper(II) ion. One of the recently reported complexes in the literature [24] characterised by single crystal X-ray crystallography exhibiting the dynamic JTE was $[Cu(OH_2)_6][BrO_3]$ (**35**), even though O–Cu–O bond angles of 90° and six equivalent Cu–O bond lengths of 2.079(4) Å were observed. X-ray crystallography (which takes an average of the entire crystal) showed clearly the operation of the dynamic JTE through analysis of the anisotropic displacement parameters in the crystal structure, which were indicative of the displacement generated by the disorder [16]. Another interesting example of the dynamic JTE in copper(II) stereochemistry is observed in $[Cu(tach)_2]^{2+}$ (**36**), where tach = *cis*,*cis*-1,3,5-triaminocyclohexane [25]. Greater than 120 K, EPR reveals the dynamic JTE in operation, with the complex oscillating between two of the three potential tetragonal elongations. Such a process, termed *the planar dynamic* JTE [26], has been reviewed at length in the comprehensive JT perspective by Falvello, who describes how structural techniques such as X-ray crystallography and EPR can still be used as probes for this effect, when analysed in a careful manner. Both $[Cu(OH_2)_6][BrO_3]$ (**35**), symmetry O_h and $[Cu(tach)_2]^{2+}$ (**36**), can be described as high symmetry systems exhibiting the dynamic JTE. Other examples of such high symmetry (O_h or D_3) systems in this dynamic JTE category are the $[Cu(NO_2)_6]^{4-}$ (**6**), and $[Cu(en)_3]^{2+}$ (**13**), systems [12]. In the origin of the vibronic coupling associated with the dynamic JTE (a_{1g} and $\pm b_{1g}$) for an octahedral CuL_6 chromophore, if a_{1g} is only in operation, the high symmetry O_h lowers to D_{4h} ($^2B_{1g}$ ground state) involving an elongated distortion (+ coupling), and also to D_{4h} ($^2A_{1g}$ ground state) involving a compressed tetragonal distortion (− coupling). A linear combination of the a_{1g} and b_{1g} modes can generate the elongated rhombic octahedral stereochemistry (except at $\theta = 60, 120, 240, 270°$). An example of a complex in the

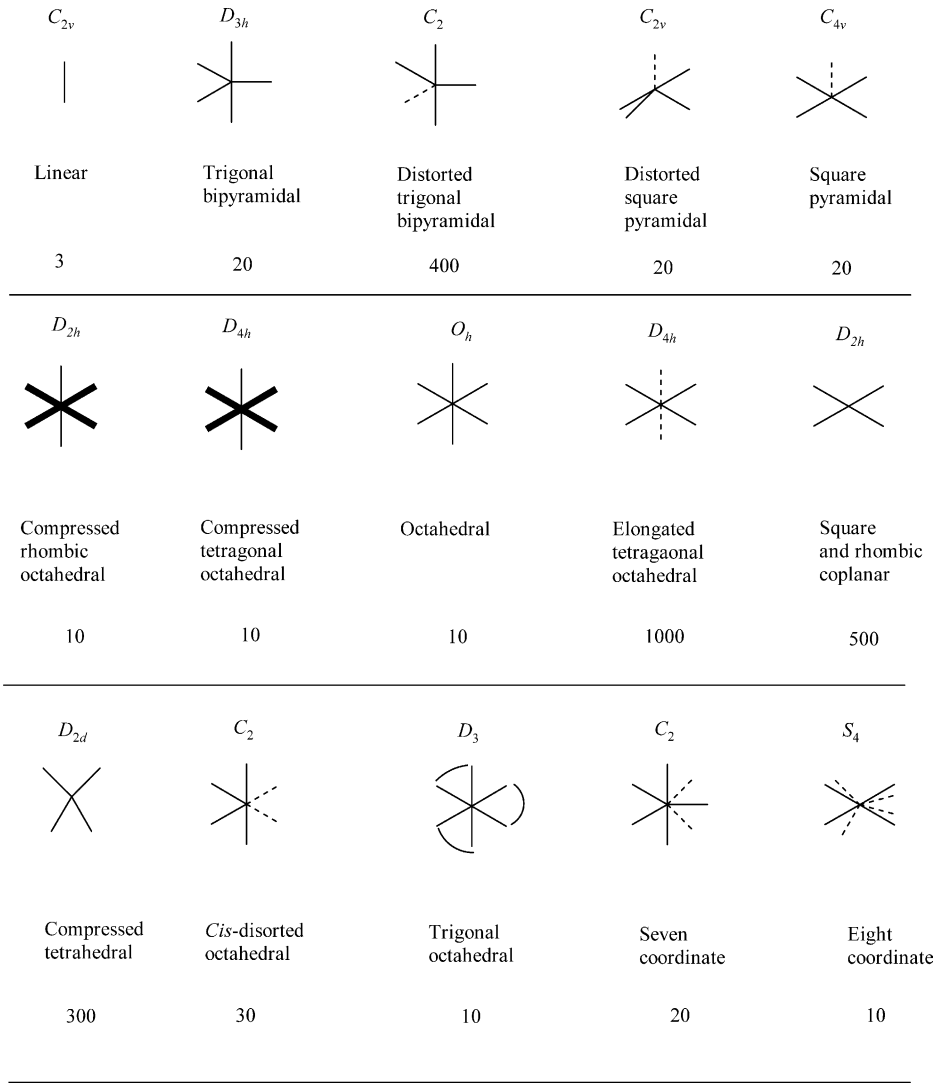

Fig. 3. A summary of the stereochemistries of the copper(II) ion, their approximate point group symmetries, their occurrence (1970): —, short bond length (1.9–2.1 Å); —, intermediate bond length (2.1–2.4 Å); – – –, long bond length (2.4–3.0 Å). (Reprinted with permission from Ref. [23]. Copyright 1970 Elsevier.)

low symmetry dynamic JTE category (D_{4h} and D_{2h} symmetries) is $[NH_4]_2[Cu(OH_2)_6][SO_4]_2$ (**21**) [27]. Overall, interest in the dynamic JTE continues to flourish in the literature, with this phenomenon thought to be involved in not only the behaviour of high-temperature superconductors [28] but also Bacci has reported from EPR studies that the spectra of specific copper blue proteins vary with temperature, linked to a dynamic JT vibronic coupling effect [29]. In a more recent publication, Beddard et al. have described the temperature dependence of the bond lengths of $[Cu(L)_2][BF_4]_2$ (L = 2,6-dipyrazol-1-ylpyridine) (**37**), using a model of dynamic JT vibronic coupling [19].

2.3. The Pseudo Jahn–Teller effect (PJTE)

In practice, the bulk of six-coordinate copper(II) complexes involve non-equivalent ligands, usually with ligands of two or three different types, CuL_4L_2' or $CuL_2L_2'L_2''$. As such systems involve a symmetry lower than O_h, the JT theory does not strictly apply and it is necessary to involve the PJTE, with symmetry mixing of a non-degenerate ground state with a non-degenerate excited state, via spin-orbit coupling [30–32]. This process, termed *vibronic coupling*, using the vibrational modes of lower symmetry, generates a range of distorted stereochemistries. As the vast majority of copper(II) complexes are of lower symmetry than O_h, the PJTE is a more appropriate starting point with which to discuss the distorted stereochemistries of the copper(II) ion. In the four coordinate regular tetrahedral stereochemistry the original JT theorem would be appropriate with an orbitally triply degenerate ground state, ^2T_u, but is redundant, as there are no known copper(II) complexes with a regular tetrahedral stereochemistry. All involve a compressed tetrahedral (CT) stereochemistry, with D_{2d}

Table 1
Examples of complexes of the different stereochemistries of the copper(II) ion and their idealised molecular symmetries

CN	Stereochemistry	Example of complex	Point group	MS	Reference
2	Linear	$CuCl_{2(g)}$	C_{2v}	**1**	[50]
4	Square and rhombic coplanar	$Ca[CuSi_4O_{10}]$	D_{2h}	**9**	[60]
4	CT	$Cs_2[CuCl_4]$	D_{2d}	**10**	[61]
5	TBP	$[Co(NH_3)_6][CuCl_5]$	D_{3h}	**2**	[51]
5	Distorted square pyramidal	$[Cu(dien)(bipyam)]Cl_2 \cdot 2H_2O$	C_{2v}	**3**	[52]
5	Square pyramidal	$K[Cu(NH_3)_5][PF_6]_3$	C_{4v}	**4**	[53]
6	Compressed rhombic octahedral	β-$[Cu(NH_3)_2Br_2]$	D_{2h}	**5b**	[54]
6	Compressed tetragonal octahedral	$Cs_2Pb[Cu(NO_2)_6]$	D_{4h}	**6**	[26]
6	Octahedral	$K_2Pb[Cu(NO_2)_6]$	O_h	**7**	[57]
6	Elongated tetragonal octahedral	$K_2Ca[Cu(NO_2)_6]$	D_{4h}	**8**	[59]
6	Elongated rhombic octahedral	$Ba_2[Cu(OH_2)_2(O_2CH)_4][HCO_2]_2 \cdot 2H_2O$	D_{2h}	**31**	[56]
6	CDO	$[Cu(phen)_2(O_2CCH_3)][BF_4] \cdot 2H_2O$	C_2	**11**	[33]
6	Asymmetric CDO (4+1+1*)	$[Cu(bipy)_2(ONO)][BF_4]$	C_1	**12**	[63]
6	Trigonal octahedral	$[Cu(en)_3][SO_4]$	D_3	**13**	[57]
7	Seven coordinate (3+2+2*)	$[Cu(py)_3(O_2NO)_2]$	C_{2v}	**14**	[64]
8	Eight coordinate (4+4*)	$Ca[Cu(O_2CCH_3)_4] \cdot 6H_2O$	S_4	**15**	[65]

CN = coordination number; MS = molecular structure.

symmetry or lower and the PJTE is more appropriate. In the five coordinate CuL_5 chromophore, few regular trigonal bipyramidal (RTBP) and regular square bipyramidal (RSBP) complexes are known, as the vast majority of five coordinate complexes involve distorted stereochemistries, generally through the presence of non-equivalent ligands. In any case, as all five coordinate copper(II) complexes involve a non-degenerate ground state, even here the PJTE is applicable and a vibronic coupling model is more relevant. Consequently, the original JT theorem really is only applicable to less than 5% of copper(II) complexes and the remaining complexes (more than 95%) are best described in terms of the PJTE or a vibronic coupling model.

In another comprehensive review [13] in 1993 on the X-ray crystallographic evidence of the role of vibronic coupling in PJT copper(II) complexes, Simmons summarised the various situations of the vibronic effects as follows (Figs. 4 and 5):

i) *A copper(II) complex without strain (already discussed)*. Here, the Jahn–Teller $E \otimes e$ vibronic coupling applies to copper(II) complexes with equivalent ligands in D_3 or O_h symmetry (warped *Mexican Hat* model).

ii) *A copper(II) complex with tetragonal strain.* If a trigonal Jahn–Teller $[Cu(chelate)_3]^{2+}$ system of D_3 symmetry (e.g. the chelate complex involving three bidentate nitrogeneous ligands), has one of the N–N ligands replaced by another chelate group (e.g. O–O), the point group lowers to C_2, the electronic degeneracy lifts, with the ^2E term splitting into the ^2A ground state and the ^2B excited state, and the e vibration splits into an a and a b mode (Fig. 4). A Jahn–Teller complex with symmetry less than O_h or D_3, as rationalised by Simmons, subject to tetragonal strain, is then termed a PJT complex. In this situation, the complex involves the PJTE with $(A \oplus B) \otimes (a \oplus b)$ vibronic coupling. If the barrier height is less than the thermal energy, kT, the two 90° misaligned chromophores become thermally accessible, generating the *pseudo* compressed octahedral stereochemistry.

iii) *A copper(II) complex with both tetragonal and orthorhombic strain*. In general, crystal packing forces alone contribute to orthorhombic strain in either JT or PJT complexes. If however, one of the O ligands is replaced by O′, as shown in Fig. 4, orthorhombic strain occurs. If a PJT complex has both tetragonal and orthorhombic strain, $(A \oplus A) \otimes (a \oplus a)$ vibronic coupling is in operation. If then ΔE is sufficiently small, the observed complex will be temperature dependent. An example of such a PJT complex is the complex $[Cu(bipy)_2(ONO)][NO_3]$ (**33**) [33–35]. The crystal structure of $[Cu(bipy)_2(ONO)][NO_3]$ (**33**), has been solved at a range of temperatures at 296, 165, 100 and 20 K, respectively. The room temperature (r.t.) crystal structure showed a *cis*-distorted octahedral (CDO) complex, with copper–oxygen bond distances at 2.230(5) and 2.320(5) Å ($Cu–O_{mean} = 2.275(5)$ Å), and a back angle α_3 [88] (Fig. 7), of 102.8(1)°. With $\Delta O = 0.090(5)$ Å at 296 K, this suggested a *fluxional* or temperature variable stereochemistry. The 20 K low temperature structure however involved an asymmetric nitrite, with copper–oxygen bonds at 2.051(2) and 2.536(2) Å ($Cu–O_{mean} = 2.294(2)$ Å, $\Delta O = 0.485(2)$ Å), with $\alpha_3 = 100.68(7)°$.

iv) *PJT $(A \oplus B) \otimes b$ vibronic coupling*. When the tetragonal strain is adequately big enough, the minimum at $\phi = 0°$ is considered to be too high in energy value to be appreciably populated at r.t. In

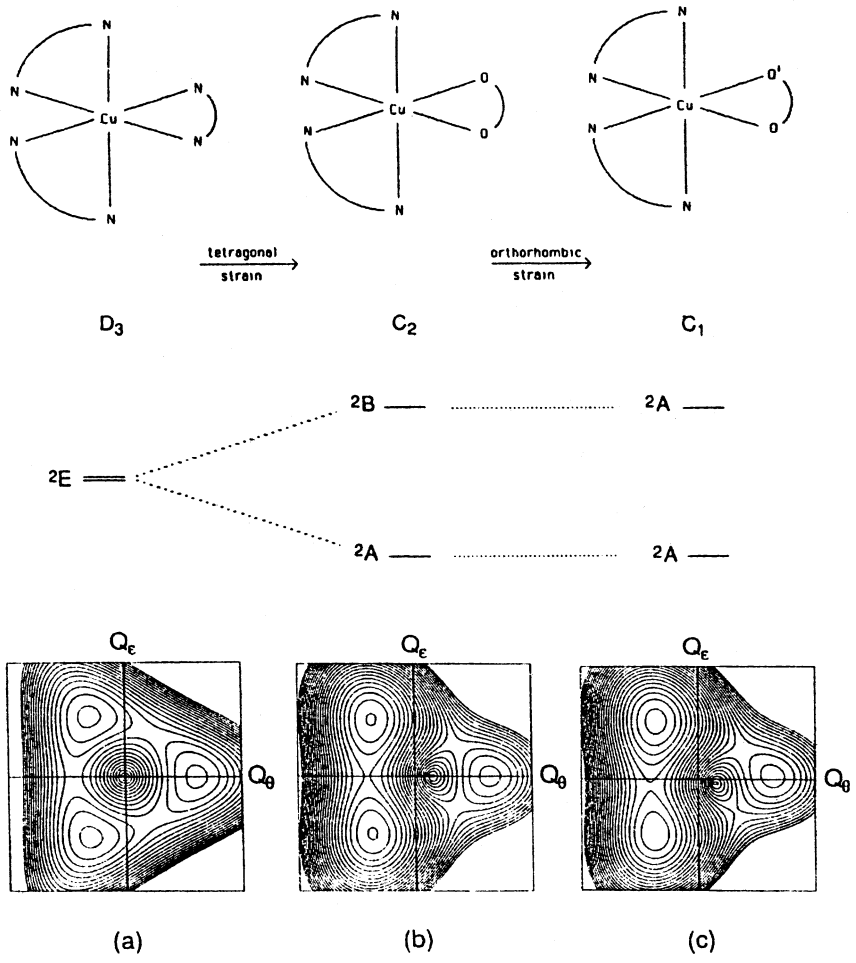

Fig. 4. Contour plots of lower energy sheets: (a) $E \otimes e$ vibronic coupling characteristic of a JT $[Cu(N-N)_3]^{2+}$ complex with no strain; (b) $(A \oplus B) \otimes (a \oplus b)$ vibronic coupling characteristic of a PJT $[Cu(N-N)_2(OXO)]^{v+}$ complex with tetragonal compression; (c) $(A \oplus A) \otimes (a \oplus a)$ vibronic coupling characteristic of a PJT $[Cu(N-N)_2(OXO')]^{v+}$ complex with tetragonal compression and orthorhombic strain (Ref. [13]. Copyright 1993. Reproduced by permission of The Royal Society of Chemistry (RSC) and the Centre National de la Recherche Scientifique (CNRS).)

such conditions, the $(A \oplus B) \otimes b$ vibronic coupling model has been suggested. The distortion has been rationalised in terms of two thermally accessible copper(II) chromophores, each with their elongation axes misaligned in two mutually orthogonal directions. Such a simple vibronic coupling model has been employed in understanding the ESR and X-ray crystallographic data of pure and doped copper(II) complexes [12,36,37].

2.4. Cooperative Jahn–Teller effect (CJTE) and the JT switch

In theory, a JT active complex in the gaseous phase is dynamic in nature and oscillates between a series of degenerate shapes. The effective energy barrier that must be traversed imposes a restriction on the populations of the actual shapes themselves. However, in the solid-state, as discussed by Falvello [16] in his review on JT effects, the CJTE occurs when the magnitude of the perturbing forces, generated by the environment in the crystal, is sufficiently strong to block the full dynamic expression of the JTE, but not big enough to suppress the distortion in its entirety. In this case, the single molecular distortion observed is an artefact of the environment in the crystal. However, the size of the distortion largely depends on the vibronic properties of the complex itself. In this sense, the CJTE as described by Falvello, is basically the trapping of distinct solid-state crystallographic manifestations of the dynamic JT effect. In other words, if the CJTE is not operative in a system, the JT active system in the solid-state could adopt random distortions and could still oscillate between the energetically degenerate shapes in the crystal. Many authors, including Bersuker and Reinen have reported how the CJTE can play a pivotal role in relation to the crystal packing of copper(II) complexes [38,39]. The CJTE can account for the highly packed arrangements often characteristic of copper(II) stereochemistries [40,41].

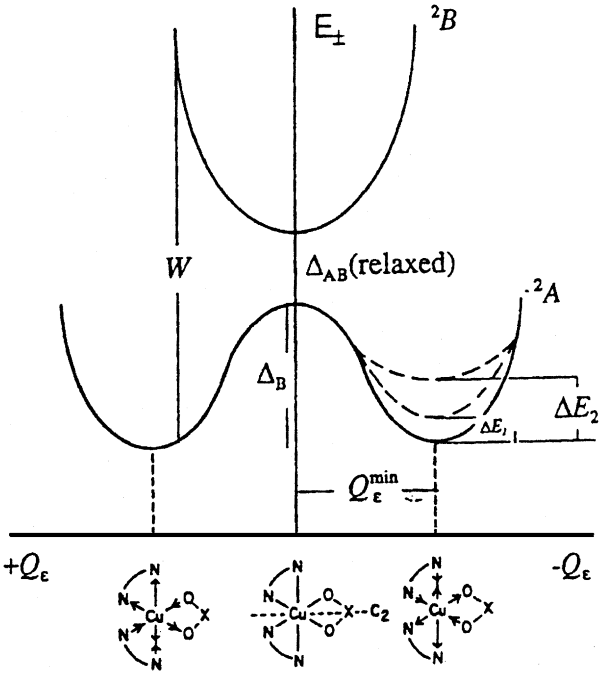

Fig. 5. Cross section through the two sheets of the $(A \oplus B) \otimes (a \oplus b)$ APES along Q_ε at Q'_θ characteristic of $(A \oplus B) \otimes (a \oplus b)$ vibronic coupling. The two minima are separated in energy by ΔE if there is orthorhombic strain, which varies for a series of cation-distortion isomers. (Ref. [13]. Copyright 1993. Reproduced by permission of The Royal Society of Chemistry (RSC) and the Centre National de la Recherche Scientifique (CNRS).)

One of the most interesting examples seen in copper(II) stereochemistry, that has been suggested to involves the CJTE from the pioneering work of Hitchman et al. involved the Tutton salt, $[NH_4]_2[Cu(OH_2)_6][SO_4]_2$ (**21a**), and its deuterated form, $[ND_4]_2[Cu(OD_2)_6][SO_4]_2$ (**21b**) [42]. In the latter form, the long axis of the CuO_6 chromophore is directed to the pair of O(8) water molecules. However, in the former, the direction is towards the O(7) group of water molecules. In addition, some alterations in the orientations and hydrogen-bonding networks of the ammonium cation and sulfate anion were observed. When the pressure was increased from ambient pressure to 1.5 kbar, there was a subsequent switch from the deuterated form to the hydrogeneous form. This is one of the best examples of a phenomenon that has been given the generic term, the Jahn–Teller Switch [42]. Schultz et al. have shown that if the pressure is decreased, a hysteresis is observed [43]. Figgis has looked at the charge density of the deuterated form [44]. In 1993, Simmons et al. did calculations on the resulting APES using tetragonal and orthorhombic strain parameters, estimated from the temperature variation of the Cu–O bond lengths [45]. Hitchman et al. in 1999, proposed a new model to explain the behaviour of the pure $[ND_4]_2[Cu(OD_2)_6][SO_4]_2$ (**21b**) [42]. The basis of this model is that the probable energy state of each individual complex is estimated after taking on board all the likely orientations of its neighbours in the lattice. The thermal behaviour is then dominated by the cooperative interactions between the individual complexes, through the hydrogen-bonding networks present. In an extension to this work, Simmons et al. in 2000, showed the effect of zinc substitution on the crystal structure of $[ND_4]_2[Cu(OD_2)_6][SO_4]_2$ (**21b**) [46]. In the pressure range, 0–400 bar at r.t., they reported essentially no change in the unit cell parameters and g-values in the EPR spectra. However, at 450 bar, once more a switch was observed to the unit cell and EPR parameters of the second form. Although they proposed no clear mechanism, they did suggest that the replacement of copper(II) with zinc(II) had an influence on the structure by its inherent effect on the packing. Unlike the iron(II) spin isomers previously reported by Jakobi et al., the main differences in structure between the two forms of ammonium copper(II) sulfate involves the packing of highly distorted complexes, which have basically identically volumes [47]. In another recent development in this area, Augustyniak-Jablokow et al., reported the continuous changes of the JT deformation of the $Cu(OH_2)_6$ complex in ferroelastic $Cs_2Cu(ZrF_6)_2 \cdot 6H_2O$ (**38**) [48]. They have stated that the gradual transformation of the complex is the first observation of the APES transformation connected with the movement of the minimum along the $\varnothing$ coordinate for $\rho \approx \rho_o$. They claim that this results from the competition between the definite low symmetry deformation of the complex existing at $T > T_c$ and the new deformation at $T = T_c$, increasing with decreasing temperature.

3. The Plasticity effect

In 1970, a review [49] of the stereochemistry of the copper(II) ion involved a rather static picture of these stereochemistries [26,33,34,50–65] (Fig. 3 and Table 1). In 1976 [66], this picture was slightly modified by the *Plasticity effect* showing how the same complex in different crystallographic modifications, had slightly different structures. The Plasticity effect was considerably extended by reference to both cation and anion distortion isomers [26,54,55,57,67–69], in which the structures of a given cation or anion are modified in the presence of different anions and cations, respectively. These effects were rationalised in the mid-1980's, in terms of the JT [38] or PJTE [35] on high symmetry structures. In this period also [12,70–72], the approach was extended to the tetrahedral and trigonal bipyramidal (TBP) stereochemistries and in 1990 all of these systems were developed by Hathaway and co-workers in terms of a vibronic coupling model [73]. Taken collectively, the proposed vibronic coupling model suggested applied to basic high symmetry systems, i.e. O_h, D_{4h},

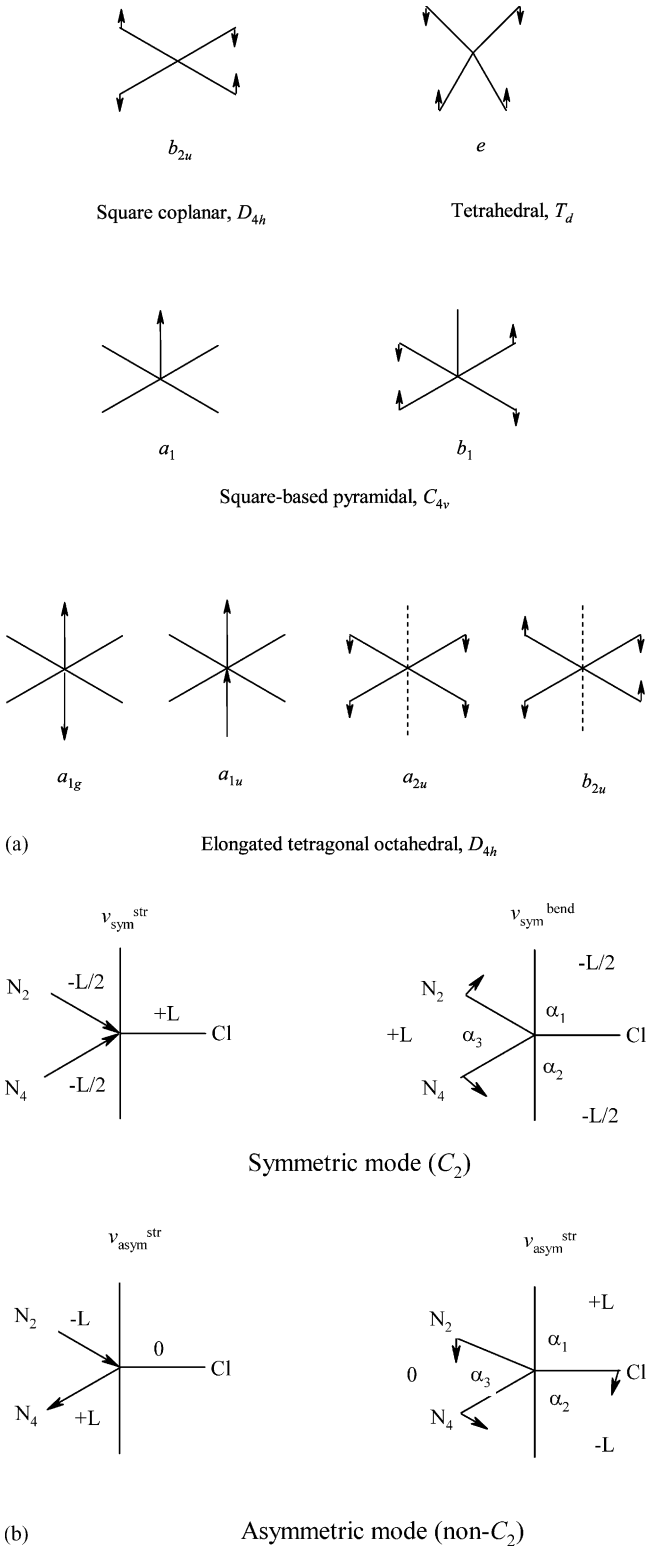

Fig. 6. (a) Selected modes of vibration for the SC, tetrahedral, square-based pyramidal and elongated tetragonal octahedral stereochemistries. (b) The symmetric and asymmetric modes of vibration for the $[Cu(phen)_2Cl]^+$ chromophore, including the relative magnitudes (L). (Ref. [75]. Copyright 1997. Reproduced by permission of The Royal Society of Chemistry.)

D_{3h} and C_2, generating temperature variable or *fluxional* systems.

However, the vibronic coupling mechanism can equally be applied to low symmetry systems such as C_1 and suggests that the original static stereochemistries of Fig. 3 are all connected, (Fig. 6(a) and (b)), and continuously variable. This has led to the graphical view of copper(II) structures, involving their respective structural pathways (described later in detail in this review) [75–78], to describe such variable stereochemistries.

In general, structural evidence for the existence of such pathways of the copper(II) ion can be obtained from two sources:

i) Different crystal forms of the same compound, e.g. α-$[Cu(NH_3)_2Br_2]$ [67] (**5a**) and β-$[Cu(NH_3)_2Br_2]$ [54] (**5b**);
ii) A series of cation or anion distortion isomers of the same cation or anion in a varying crystal environment of the counter anion or cation, respectively, e.g. the $[Cu(bipy)_2Cl]^+$ cation, **18**, **19**, of which 18 structures are currently known [78].

The structural data may then be involved in:

i) A range of slightly different modifications of the same basic stereochemistries e.g. the $[Cu(OH_2)_6]^{2+}$ cation, **20**, **21**, with an elongated tetragonal or rhombic octahedral (EO) stereochemistry [79,80].
ii) A range from one stereochemistry to another e.g. the $[Cu(NH_3)_4X_2]$ [81,82] series ranging from elongated tetragonal to square coplanar (SC) stereochemistries, **22**, **23**.

All of these continuously variable stereochemistries can be characterised by X-ray crystallography and can be qualitatively understood broadly terms of JT phenomena and vibronic coupling.

However, when a sufficiently large data set is available [73,75–78], as in the 18 structures of the $[Cu(bipy)_2Cl]^+$ cation [78] (Table 2), scatter plot analysis may be used to probe for correlations in the CuN_4X chromophore structures. In 1999 [78], scatter plot analysis was used to advocate the existence of correlations between the in-plane modes of vibration of the CuN_2Cl chromophore. In general, the data points of the scatter plots are not random but suggest parallel trend lines. To account for the occurrence of linear plots, progressions of the individual modes of vibrations, ν_{sym}^{str}, ν_{sym}^{bend}, ν_{asym}^{str} and ν_{asym}^{bend}, are required and as in C_1 symmetry all four modes transform as A_1, and a linear progression and combination of all four modes is required to account for the directions of the trends. This suggests that the scatter plots themselves represent a cross section of the vibronic potential energy surface (PES), with the minimum of the surface located at the data points and each characterised by a crystal structure determination.

Four coordinate complexes

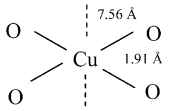

$Ca[CuSi_4O_{10}]$,[60] **9**

Square coplanar

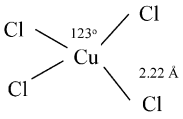

$Cs_2[CuCl_4]$,[61] **10**

Compressed tetrahedral

Five coordinate complexes

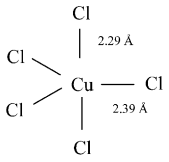

$[Co(NH_3)_6][CuCl_5]$,[51] **2**

RTBP

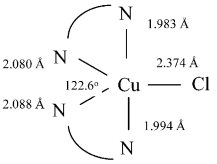

$[Cu(bipy)_2Cl][OH].6H_2O$,[71] **19**

$\tau = 1.00$

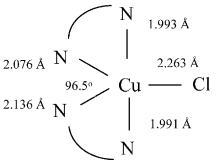

$[Cu(bipy)_2Cl][ClO_4]$,[70] **18**

$\tau = 0.62$

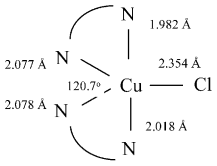

$[Cu(bipy)_2Cl].1/2OH.1/2Cl$,[96] **32**

$\tau = 0.97$

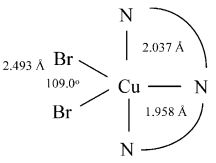

$[Cu(terpy)Br_2]$,[114] **30**

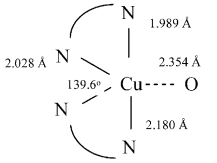

$[Cu(phen)_2(OH_2)][NO_3]$,[62] **34**

$\tau = 0.53$

Six coordinate complexes

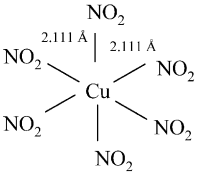

$K_2Pb[Cu(NO_2)_6]$,[57] **7**

Regular octahedral

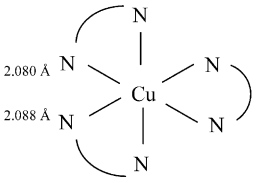

$[Cu(en)_3][SO_4]$,[57] **13**

Trigonal octahedral

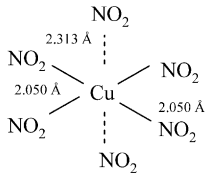

$K_2Ca[Cu(NO_2)_6]$,[59] **8**

Elongated tetragonal octahedral

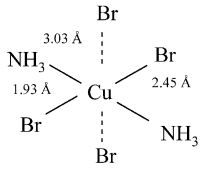

α–$[Cu(NH_3)_2Br_2]$,[67] **5a**

Elongated rhombic octahedral (A-type distortion isomer)

Fig. 7. Selected examples of complexes of copper(II) complexes of coordination numbers 4, 5 and 6, respectively.

Six coordinate complexes

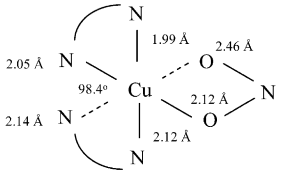

[Cu(bipy)$_2$(ONO)][BF$_4$],[63] **12**

Asymmetric *cis*-distorted octahedral

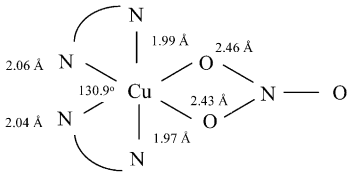

[Cu(phen)$_2$(O$_2$NO)][NO$_3$],[89] **26a**
(Green)

Near regular bicapped square pyramidal

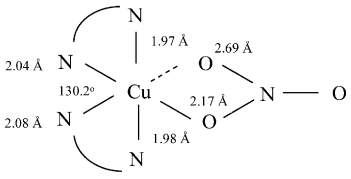

[Cu(phen)$_2$(O$_2$NO)][NO$_3$].CH$_3$OH,[89] **26b**
(Blue)

Asymmetric distorted bicapped square pyramidal

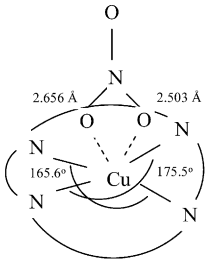

[Cu(MeTAAB)(O$_2$NO)][NO$_3$],[90] **27**

Regular bicapped square pyramidal

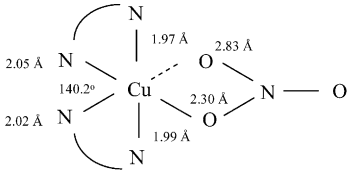

[Cu(bipy)$_2$(O$_2$NO)][NO$_3$].H$_2$O,[91] **28**
(Blue)

Distorted bicapped square pyramid (4 + 1 + 1*)

Fig. 7 (*Continued*)

4. Summary of the simple systems available

In each of the following groups extensive series of copper(II) complexes of known crystal structure are involved. A selection of some of the structures of the individual complexes are shown in Fig. 7.

Category I Type: [Cu(NH$_3$)$_4$X$_2$], [81,82] **22**, **23** and [Cu(en)$_2$X$_2$], [83,84] **24**, **25** complexes.

The stereochemistries of these complexes range from elongated tetragonal or rhombic octahedral, (EO), to square (SC) or rhombic coplanar. All involve static stereochemistries, which are not complicated by fluxional behaviour.

Category II *Type:* M$_2$[Cu(OH$_2$)$_6$]X$_2$ complexes, [79] [80] **20**, **21**.

The stereochemistries of these complexes range from elongated tetragonal or rhombic octahedral and some of the complexes are complicated by fluxional behaviour and do not involve a genuine static behaviour.

Category III *Type:* M$_2$M′[Cu(NO$_2$)$_6$] complexes, [26,55,57,59,69] **6**, **7**, **17**.

The stereochemistry of these systems vary from regular octahedral to elongated tetragonal or rhombic octahedral. The high symmetry systems are complicated by fluxional behaviour, with the cubic octahedral complexes providing some excellent examples of the operation of the dynamic JTE [16].

Category IV *Type:* M$_2$[CuCl$_4$] complexes, [61] **10**.

The stereochemistry of these complexes vary from compressed tetrahedral (CT), to square and rhombic coplanar. They display no evidence of fluxional behaviour.

Six coordinate complexes

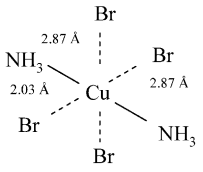

β–[Cu(NH$_3$)$_2$Br$_2$],[54] **5b**

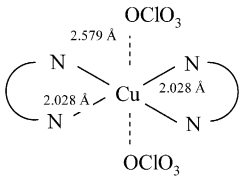

α–[Cu(1,3 diaminobutane)$_2$(ClO$_4$)$_2$],[68] **16a**
(Blue-violet)

Compressed tetragonal octahedral
(A-type distortion isomer)

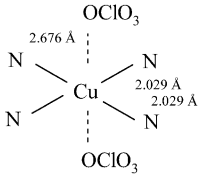

β–[Cu(1,3 diaminobutane)$_2$(ClO$_4$)$_2$],[68] **16b**
(Red-violet)

Elongated tetragonal octahedral
(B-type distortion isomer)

Elongated tetragonal octahedral
(B-type distortion isomer)

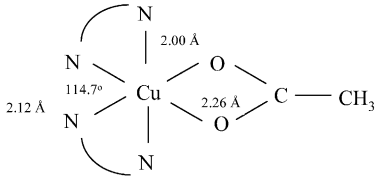

[Cu(phen)$_2$(O$_2$CCH$_3$)$_2$][BF$_4$].2H$_2$O,[33] **11**

***Cis*-distorted octahedral**

Fig. 7 (*Continued*)

Category V *Type:* [Cu(chelate)$_2$X]Y complexes.

The stereochemistry of these five coordinate complexes vary from RTBP, e.g. $[CuCl_5]^{3-}$, D_{3h} symmetry [51], to distorted square (DSBP) or rhombic base pyramidal, e.g. [Cu(bipy)$_2$Cl]Y, C_1 symmetry [78]. Fluxional behaviour has been suggested in the high symmetry $[CuCl_5]^{3-}$ anion, but all the complexes of the corresponding [Cu(bipy)$_2$Cl]Y series are static [78,85], even near the RTBP stereochemistry, possibly attributed to the energy involved in moving the heavy chloride ligand.

Category VI *Type:* [Cu(chelate)$_2$(OXO)]Y complexes.

The stereochemistry of the CuN_4O_2 chromophore in these CDOs, vary from the highest symmetry of C_2, as seen in $[Cu(phen)_2(O_2CCH_3)][BF_4] \cdot 2H_2O$ [33,34] (**11**), to the absence of symmetry, C_1, as seen in [Cu(bipy)$_2$(ONO)][BF$_4$] [86] (**12**), in the [Cu(bipy)$_2$(ONO)][Y] series [63] with a very asymmetrically bonded $(ONO)^-$ anion (Table 3). The latter complex is best described as a five coordinate square bipyramidal (SBP) stereochemistry with off z-axis coordination generating a 4+1+1* structure. The C_2 and near C_2 complexes are subject to fluxional behaviour, probably due to the lightness of the ONO^- anion and the small distance that it has to move [63,86–88]. The extreme 4+1+1* structures are non-fluxional. As the presence of fluxional behaviour invalidates the structure as a genuine static stereochemistry of the copper(II) cation, these are referred to as *pseudo* stereochemistries.

5. Overview of the principle of structure correlation analysis in chemistry

The relationship between chemistry and structure determination is well documented in the literature [74,93,94]. Rapid progress is being made in developing new tools to understand structure. The use of X-rays, electron microscopes and nuclear reactors are among the many physical and chemical techniques available to researchers working in the area of structural science. One of the most important tools in this domain, involves computational studies where structures can be calculated and visualized in three-dimensions. In 1997, Hoffmann [94] stated that 'there is no more basic enterprise in chemistry than the determination of the geometrical structure of a molecule. Such a determination when it is well done, ends speculation and provides us with the starting point for the understanding of every physical, chemical and biological properties of the molecule.' As advances in X-ray crystallography continue to thrive at an incredible rate, databases of

Six coordinate complexes

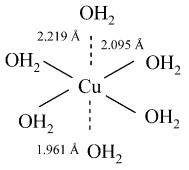

$(NH_4)_2[Cu(OH_2)_6](SO_4)_2$,[42,80] **21**

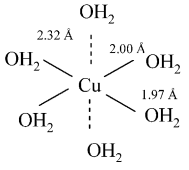

$Cs_2[Cu(OH_2)_6](SO_4)_2$,[79] **20**

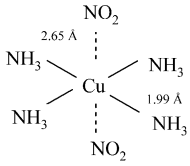

$[Cu(NH_3)_4(NO_2)_2]$,[81] **22**

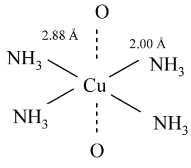

$Na_4[Cu(NH_3)_4][Cu(S_2O_3)_2].H_2O$,[82] **23**

Fig. 7 (*Continued*)

thousands of isolated crystal structures has led to a new emerging field in chemistry, involving structure systematics, called comparative X-ray crystallography [75–78,93]. Using the biological analogy of the infamous ant colony, it is clear that if the nature and fabric of the ant colony itself is to be explored, one, single ant of the colony should not be examined in isolation, but rather the entire colony must be considered.

At the core of this new field of chemistry is the idea of structure correlation analysis [95,96]. As Bürgi (1998) commented in his paper [93] on the relationship between the chemical properties, structure and X-ray crystallography, by having the capacity to visualize the actual architecture of matter at the atomic level can lead to a more in-depth understanding of the chemical phenomena involved. If a structural database of a series of closely related molecules or fragments is available, it is nowadays possible to infer details of geometrical variations occurring along certain defined reaction pathways. The structure correlation hypothesis [96,97] states that the geometric changes a given molecular fragment undergoes along a specific reaction coordinate, are mirrored by the gradual distortion or static deformation manifested by that fragment collectively over a large variety of crystalline environments. In this vein, structure correlation analysis can potentially extract not only just core structural information but also can be used as a structural probe within this body of information and can even help us to visualize the actual modes of vibration in operation [75–78], which cannot be derived from an isolated crystal structure determination, as in the analogy of the ant colony in biology. Collectively, structure correlation analysis, chemical structure modeling and quantum chemistry can open a door into the molecular design of materials with specific properties and characteristics, and can act as a probe for studying complex geometrical systems. It is this combination of tools that the true secrets and the intrinsic beauty of structure can be revealed and forms one of the most powerful bridges linking coordination chemistry, materials science and crystal engineering in science. Structure correlation analysis can involve the mapping of a reaction pathway, during the course of a chemical reaction, the correlation between structure and catalytic behaviour, structure and magnetic properties, structure and the rate of a chemical reaction, structure and energetics and structure and electronic properties [93].

Structure correlation involves two distinct areas: structure–property correlations and structure–structure correlations, which is the correlation of interatomic bond lengths and angles. The basis of the structure correlation hypothesis is that an individual crystal structure (in a series of closely related molecular fragments) represents a point in a regional cluster of low potential energy, along a pathway of minimum energy, PES. As a crystal structure represents a stable atomic arrangement, its point on the Born-Oppenheimer PES will have a tendency to cluster around local potential minima, which can be a point in a valley or a well [96]. Consequently, the individual crystal structure points in the series represent a '*snapshot*' taken along the reaction pathway, and when viewed cooperatively in sequence represents a cinematic picture of the path of the reaction.

Table 2
Selected bond lengths and angles for the $[Cu(bipy)_2Cl][Y]$ series of cation distortion isomers

	α_1 (°)	α_2 (°)	α_3 (°)	Cu–Cl (Å)
$[OH]^- \cdot 6H_2O$, **19**	118.7(3)	118.7(4)	122.6(4)	2.374(5)
$[PF_6]^- \cdot H_2O$, **39**	115.7(2)	120.5(2)	123.8(2)	2.344(2)
$Cl^- \cdot 6H_2O$, **40**	118.7(3)	118.6(3)	122.8(4)	2.361(4)
$[^1/_2OH \cdot {}^1/_2Cl]^-$, **32**	119.0(6)	120.2(6)	120.7(7)	2.354(8)
$[(CH_3)_2C_6H_3SO_3]^- \cdot H_2O$, **41**	118.6(1)	121.6(1)	119.8(1)	2.337(1)
$[NO_3]^- \cdot 3H_2O$, **42**	127.8(2)	123.4(2)	108.8(2)	2.308(3)
$^1/_2[S_5O_6]^- \cdot 6H_2O$, **43**	130.7(1)	122.0(2)	107.3(2)	2.292(4)
$[CuCl_2]^- \cdot C_6O_6H_4$, **44**	131.7(1)	121.1(1)	107.1(1)	2.294(1)
$[CuCl_2]^-$, **45**	133.4	111.1	115.5	2.356
$[BF_4]^-$, **46**	134.8(3)	127.6(3)	97.6(3)	2.285(3)
$[CF_3SO_3]^- \cdot H_2O$, **47**	133.1(1)	119.9(1)	106.9(1)	2.259(1)
$[MoS_4Cu_2Cl_3]$, **48**	134.0(2)	119.8(2)	106.2(2)	2.273(3)
$[ClO_4]^-$, **18**	137.1(1)	126.4(2)	96.5(2)	2.263(3)
$[WS_4Cu_2Cl_3]^-$, **49**	136.2(2)	121.1(2)	102.6(3)	2.275(3)
$[CF_3(CF_2)_3SO_3]^-$, **50**	136.8(2)	119.2(2)	104.0(2)	2.284(2)
$[(NC)_5C_2]^-$, **51**	138.5(2)	114.2(2)	107.3(3)	2.277(3)
$[(CN)_4(quin)]^-$, **53**	135.6	116.0	108.4	2.301
$[CF_3SO_3]^- \cdot H_2O$, **54**	140.4(1)	119.1(1)	100.6(1)	2.246(2)
	Cu–N(1) (Å)	Cu–N(2) (Å)	Cu–N(3) (Å)	Cu–N(4) (Å)
$[OH]^- \cdot 6H_2O$, **19**	1.983(11)	2.080(12)	1.994(11)	2.088(13)
$[PF_6]^- \cdot H_2O$, **39**	1.996(6)	2.105(6)	2.005(6)	2.108(6)
$Cl^- \cdot 6H_2O$, **40**	1.989(10)	2.077(21)	1.970(10)	2.087(10)
$[^1/_2OH \cdot {}^1/_2Cl]^-$, **32**	1.982(19)	2.077(21)	2.018(19)	2.078(21)
$[(CH_3)_2C_6H_3SO_3]^- \cdot H_2O$, **41**	1.982(3)	2.093(2)	1.988(3)	2.101(2)
$[NO_3]^- \cdot 3H_2O$, **42**	1.989(6)	2.089(6)	1.989(6)	2.112(5)
$^1/_2[S_5O_6]^- \cdot 6H_2O$, **43**	1.992(6)	2.092(6)	1.988(6)	2.106(5)
$[CuCl_2]^- \cdot C_6O_6H_4$, **44**	1.991(3)	2.071(3)	1.988(3)	2.104(3)
$[CuCl_2]^-$, **45**	1.985	2.063	1.995	2.086
$[BF_4]^-$, **46**	2.006(7)	2.079(8)	1.983(7)	2.142(8)
$[CF_3SO_3]^- \cdot H_2O$, **47**	1.986(5)	2.091(4)	1.973(4)	2.128(3)
$[MoS_4Cu_2Cl_3]$, **48**	1.981(8)	2.076(8)	1.978(8)	2.124(8)
$[ClO_4]^-$, **18**	1.993(4)	2.076(3)	1.991(4)	2.136(5)
$[WS_4Cu_2Cl_3]^-$, **49**	1.979(8)	2.071(8)	1.973(8)	2.139(8)
$[CF_3(CF_2)_3SO_3]^-$, **50**	1.993(6)	2.061(6)	1.969(6)	2.140(6)
$[(NC)_5C_2]^-$, **51**	1.969(8)	2.062(9)	1.998(8)	2.118(8)
$[(CN)_4(quin)]^-$, **53**	1.990	2.066	1.904	2.126
$[CF_3SO_3]^- \cdot H_2O$, **54**	1.981(4)	2.083(4)	1.995(4)	2.140(4)

5.1. Examples

Structure correlation analysis has been employed in several studies in chemistry. Perhaps one of the best known studies was by Bürgi in 1973 [98], on the reaction pathway of the ligand exchange reaction $XCdS_3 + Y \rightarrow X\cdots CdS_3\cdots Y \rightarrow X + S_3CdY$ from X-ray data of five coordinate cadmium complexes. The correlations that transpired described the structural pathway of the reaction. As the reaction progressed, the tetrahedral $XCdS_3$ species has a potential fifth Y ligand on the face of the tetrahedron, *trans* to ligand X. Bürgi reported that the CdS_3 pyramid was found to flatten as Y approached it and X shifted away from the cadmium centre. The cadmium lied in the same plane as the three sulfurs once Δx and Δy are equivalent. It was found that the closer Y was to the cadmium, the further X drifted away, eventually forming the S_3CdY complex, with inversion of the CdS_3 pyramid, similar to the sequence of structural changes thought to occur during a bimo-

Table 3
Selected bond lengths and angles for the $[Cu(bipy)_2(ONO)][Y]$ series of cation distortion isomers

	$[Cu(bipy)_2(ONO)][Y]$ series [13,35,87,92]			
	α_3 (°)	Cu–O(1) (Å)	Cu–O(2) (Å)	ΔO (Å)
$[PF_6]^-$, **55**	115.5(1)	2.178(5)	2.429(5)	0.251(5)
$[I]^-$, **56**	105.2(3)	2.203(8)	2.266(7)	0.063(8)
$[NO_3]^-$ (296 K), **33**	102.8(1)	2.230(5)	2.320(4)	0.090(5)
$[NO_3]^-$ (20 K), **57**	100.68(7)	2.051(2)	2.536(2)	0.485(2)
$[BF_4]^-$, **58**	98.5(2)	2.117(6)	2.463(6)	0.346(6)
$[ClO_4]^-$, **60**	97.9(3)	2.087(9)	2.492(9)	0.405(9)
$[HSO_4]^-$, **59**	97.24	2.026	2.569	0.549

lecular nucleophilic displacement SN2 reaction in organic chemistry. In this analysis, in order to describe the continuous transition from tetrahedral to TBP stereochemistry, one additional structural parameter was considered to generate a three-dimensional parameter space. This was chosen to be the $\langle X\hat{M}S \rangle$, which displayed a continuous change from $>90^\circ$ to $<90^\circ$ with the cleavage of the X–Cd bond and the formation of the Cd–Y bond. It was found theoretically that quantum chemistry yielded similar results.

Another example of an early study [99] involved some crystal structures of $SbCl_3$, where the coordination number of the antimony was found to be six, by the addition of three additional chlorides, generating a distorted octahedron. It was shown that the scatter plot of the short Sb–Cl bond *trans* to the longer Sb···Cl′ distances displayed a hyperbolic form, also found for I_3^- [99].

Structure correlation analysis as a structural tool has also been used extensively in organic chemistry. One such example [100] is the nucleophilic addition of an amine to the carbonyl group:

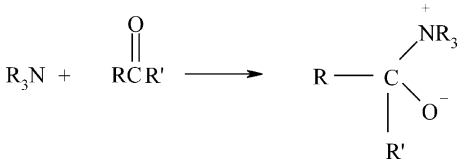

It was found that the planar carbonyl adopted a pyramidal geometry on approach of the amine at approximately the angle of a tetrahedron. The CO bond length increased until an intermediate four-coordinate tetrahedron was formed. Scatter plot analysis, involving plots of Δ versus d(N···C=O), Δ versus d(H···C=O) and projection of the RCOR′(NR_3) group onto the N···C=O plane, were considered as a series of snapshots along the continuous reaction path of the nucleophilic addition reaction. The pathway has been shown to be in agreement with the accepted mechanism for the reaction.

Other examples of structure correlation analyses can be found in recent reviews (and references therein) by Bürgi (1998) [93] and Auf der Heyde (1994) [96], including correlation studies on linear and bent OXO-bridged transition metal dimers, both homo- and heteronuclear species; coordination polymers (for use in magnetic materials); metal cluster rearrangements (Au_2Ru_3 fragments); examples from catalysis (Cp_2ZrL_3) (stereospecific polymerizations of α-olefins with a route to synthesizing and characterizing edge-bridged tetrahedral in order to probing their potential catalytic behaviour) etc.

Probably, one of the best examples of structure correlation analysis however, which is now cited in most modern inorganic chemistry textbooks involves the Berry Twist mechanism, which has led to the explanation of the equivalence of the five fluorine atoms in the NMR signal of PF_5 [101]. PF_5 adopts a TBP geometry and even at low temperature, only one type of fluorine nucleus is observed in the NMR spectrum. This has been rationalized by a Berry Twist mechanism in which there is a rapid intramolecular exchange between the equatorial and axial fluorines. In the Berry Twist mechanism, the PF_5 molecules change from the TBP stereochemistry of D_{3h} symmetry to the square-based pyramidal stereochemistry of C_{4v} symmetry as a transition state and back to D_{3h} symmetry. The resultant NMR spectrum features a single peak, as opposed to two different signals, corresponding to the sets of equatorial and axial fluorines as predicted. In a review by Holmes in 1980 [101], structure correlation was carried out on variations in bond angle with data from structures from a large data set of five-coordinate phosphorus containing compounds. Evidence of the Berry Twist mechanism has also been proven from quantum mechanics and empirical force-field calculations. Alvarez and Llunell in 2000, have extended the Berry Twist mechanism to a more detailed structure correlation, generating several different distortion modes for a TBP AX_5 fragment [58].

6. Structural pathways of the copper(II) ion

The concept of applying structure correlation methods to JT active complexes of copper(II) is consistent with what is reported in the literature about the JTE in copper(II) compounds [75–78]. This is essentially a dynamic phenomenon, and when studied in the crystalline state gives rise to a series of structures displaying the variability of molecular shape along what is termed structural pathways. These pathways are basically a set of thermally accessible molecular shapes through which a JT system can course, when present in a suitably permissive crystalline environment. They constitute furthermore, a subset of all of the possible shapes through which such a molecule would course in the gas phase. In this sense, the continuously variable stereochemistries of the copper(II) ion, (Fig. 3), are connected by the appropriate modes of vibration of the local molecular chromophore, (Fig. 6). These generate the four structural pathways of Fig. 8.

6.1. Five coordinate systems

The five coordinate Structural Pathway, involving the RTBP stereochemistry, D_{3h} symmetry, is limited to the $[CuX_5]^{3-}$ anions, distorting to the RSBP stereochemistry, C_{2v} symmetry. The five coordinate Structural Pathway is most often discussed in terms of the more informative [Cu(chelate)$_2$X]Y series of complexes (Fig. 8(c) and Fig. 9(a)). The highest symmetry of the CuN_4Cl

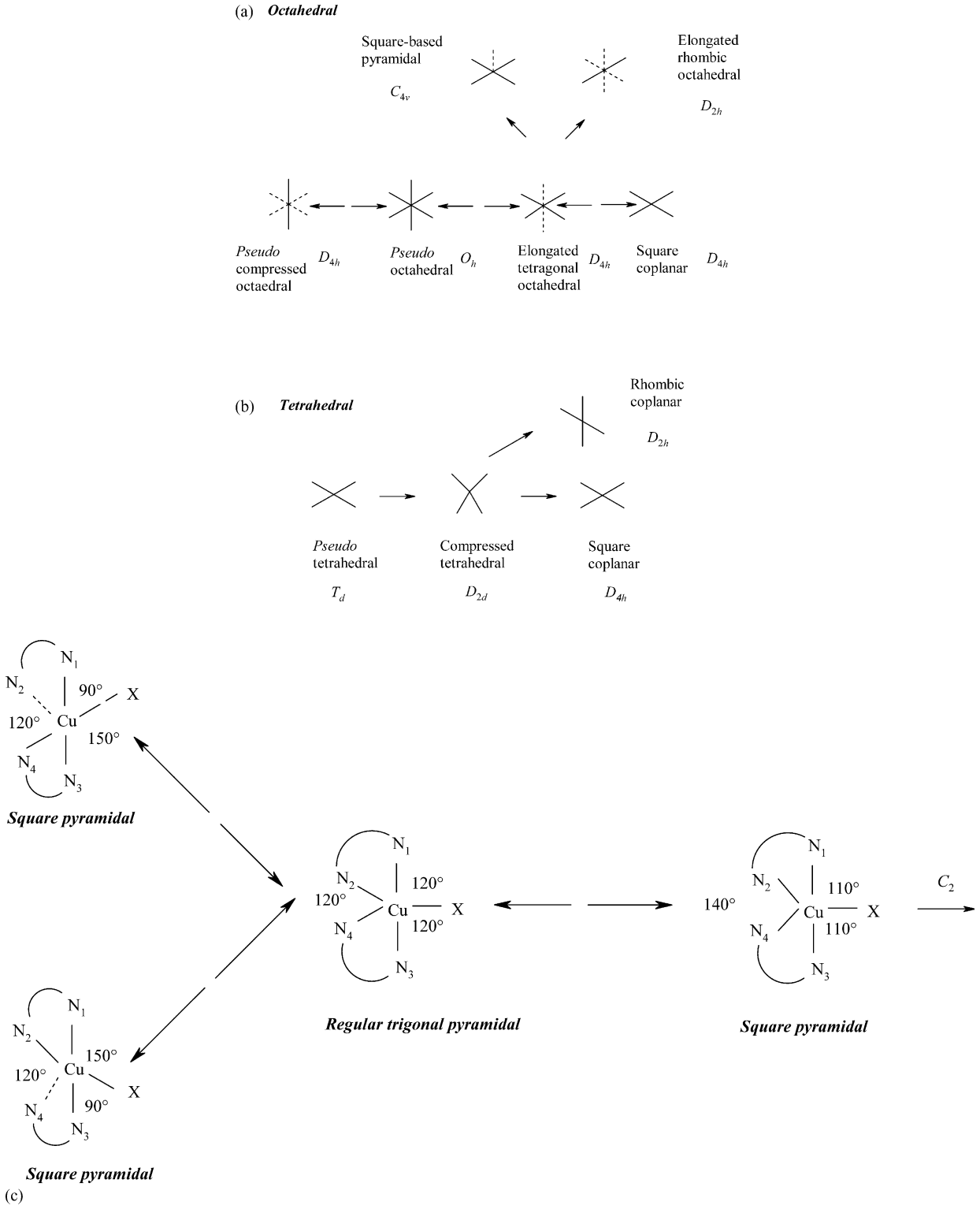

Fig. 8. (a) and (b) The structural pathways for the octahedral and tetrahedral stereochemistries of the copper (II) ion. (c) The structural pathways for the distortion of the CuN_4X chromophore from trigonal bypyramidal to square pyramidal, involving three alternative routes (Ref. [73]. Copyright 1990. Reproduced by permission of The Royal Society of Chemistry.) (d) The structural pathways for the distortion of the CuN_2N_2'OO' chromophore from CDO to distorted square pyramidal to distorted bicapped square pyramidal. (Ref. [91]. Copyright 1981. Reproduced by permission of The Royal Society of Chemistry.)

chromophore is then C_2 restricted to the horizontal axis through the RTBP stereochemistry in the +A and −A route directions, by the ν_{sym}^{str} and ν_{sym}^{bend} modes of vibration, structures **I**–**V** (Fig. 9(a)). The +A route distortion

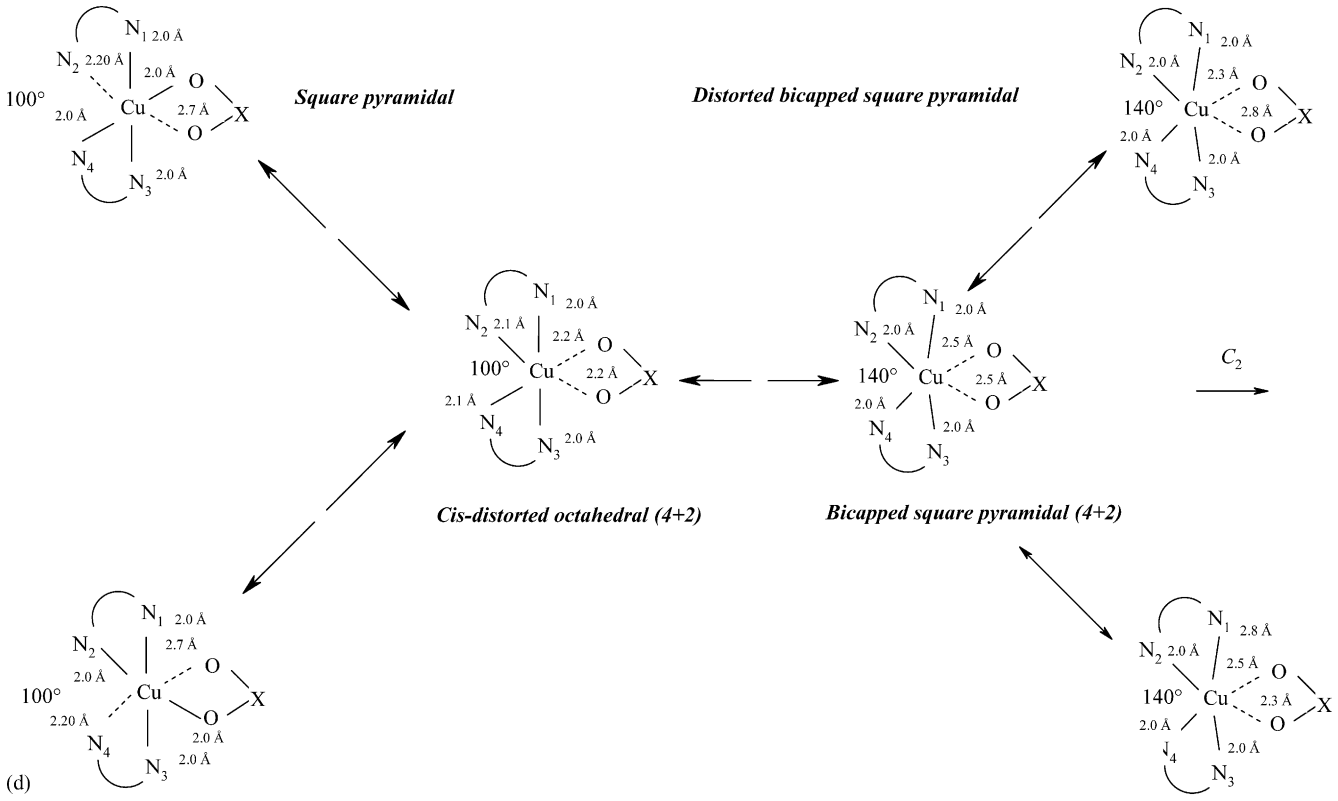

Fig. 8 (*Continued*)

is referred to as the *Forward normal* distortion and the −A route is referred to as the *Reverse* distortion. Above and below this horizontal axis, the C_2 is lowered to C_1 symmetry by the +B and −B route distortions, generated by the ν^{str}_{asym} and ν^{bend}_{asym} modes of vibration, respectively.

The A and B routes, according to the general schematic diagram in Fig. 9(a) can be summarised as follows for clarity:

+ A route: the back-angle, α_3 (e.g. the N(2)–Cu–N(4) bond angle), increases from 120° up to a maximum value of 160°, the C_2 axis of symmetry is retained and the Cu–X bond length elongates from ca. 2.3 to 2.5 Å. The overall route takes the RTBP stereochemistry through the square based distorted trigonal bipyramidal (SBPDTBP) and trigonal bipyramidal distorted square based pyramidal (TBPDSBP) stereochemistries.

−A route: the back-angle, α_3 (e.g. the N(2)–Cu–N(4) or O(2)–Cu–O(4) bond angles), decreases from 120° down to as far as 80°, the C_2 axis of symmetry is retained and the Cu–X bond length decreases from ca. 2.3 to 2.0 Å.

+B route: α_1 (the N(2)–Cu–X bond angle), increases from 120° up to a maximum value of 135°, the C_2 axis of symmetry is destroyed and the Cu–N(4) bond length elongates from ca. 2.10 to 2.15 Å.

−B route: α_1 (the N(2)–Cu–X bond angle), decreases from 120° down to a minimum of 105°, the C_2 axis of symmetry is destroyed and the Cu–N(2) bond length elongates from ca. 2.10 to 2.15 Å. The +B and −B routes are themselves related by a C_2. It should be remarked however that the α_3 bond angle, does not vary in the + or −B routes but maintains its parent 120° value.

In these four ±A and ±B route distortions, the SBDTBP stereochemistry is first generated within the α_3 range of 120–140°. Beyond this range, the stereochemistries are best described as SBP, or TBPDSBP. In the special case of the −A route distortion, with $\alpha_3 = 100$–120°, the stereochemistries have been referred to as a *Reverse* trigonal bipyramid (RevTBP), while in the range of $\alpha_3 = 80$–100°, the term *See-Saw* stereochemistry has been introduced.

In the full range of $\alpha_3 = 80$–160°, a C_2 axis of symmetry is generally maintained by the symmetric modes of vibration, ν^{str}_{sym} and ν^{bend}_{sym}. However, there is no reason why the asymmetric modes of vibration, ν^{str}_{asym} and ν^{bend}_{asym}, should not couple as they are all of A_1 symmetry in the C_1 point group. Thus, in the [Cu(bipy)$_2$Cl]Y series [78] the −A+B route distortion is appropriate, with no pure −A route distortion and α_3 in the range 98–100°. Interestingly, some of the

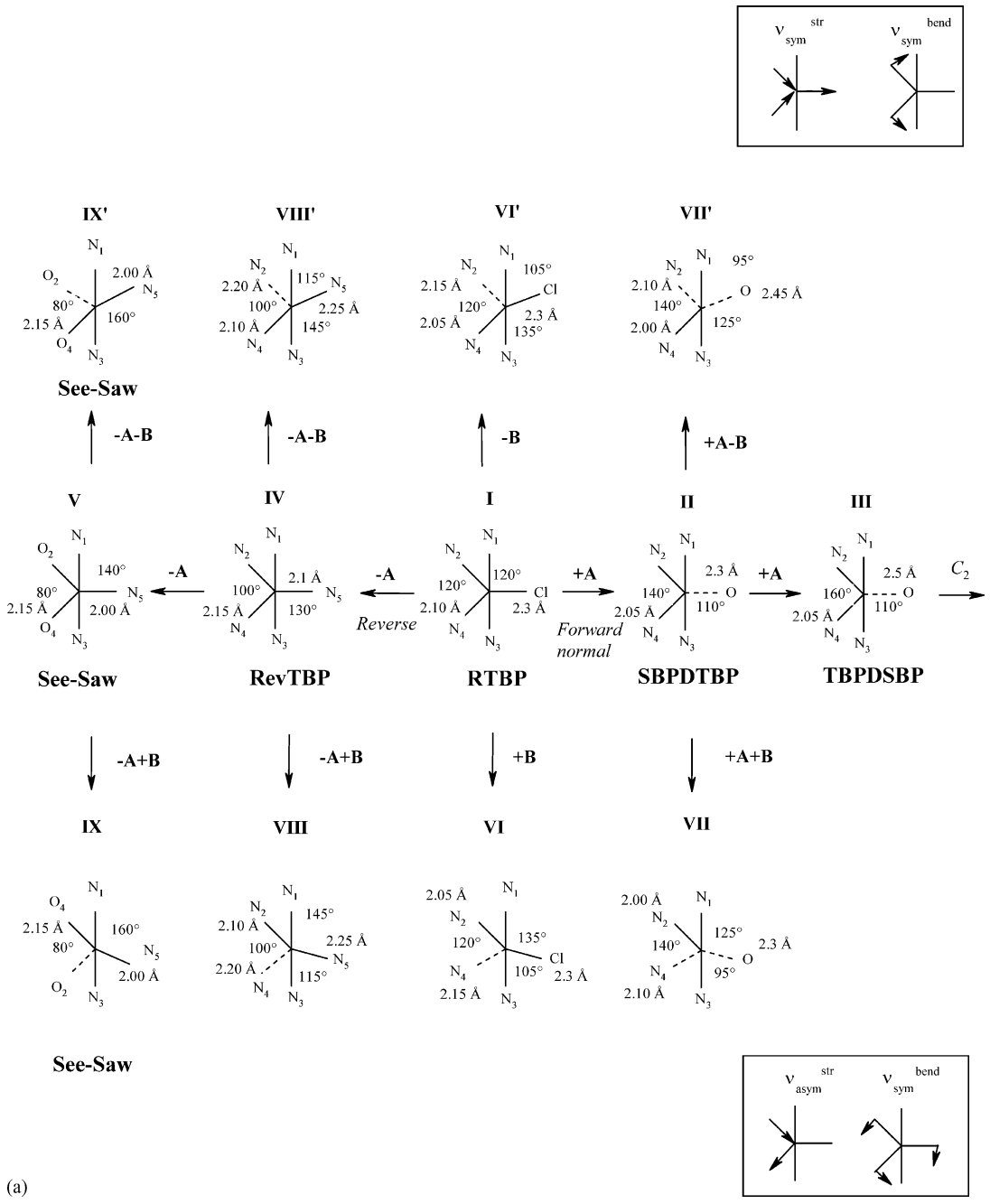

Fig. 9. (a) The structural pathways of the RTBP CuN_4X chromophore, involving the ±A, ±B and ±A±B route distortions. The bond distances have been approximated to the nearest 0.05 Å and the bond distances to the nearest 5°. (Ref. [75]. Copyright 1997. Reproduced by permission of The Royal Society of Chemistry.); (b) The structural pathways of the *cis*-distorted (CDO) CuN_4O_2 chromophore, involving the ±A, ±B and ±A±B route distortions.

$[Cu(bipy)_2Cl]Y$ complexes (Table 2) do have a near RTBP stereochemistry that might suggest possible fluxional behaviour. However, recent low temperature crystal structure determination work by the current authors [85] confirmed the absence of any temperature variability.

Described in this way the Structural Pathway for the five coordinate stereochemistry of the copper(II) cation contains a great deal of information, expressed in a graphical form, on how this stereochemistry is connected to the four in-plane modes of vibration of the CuN_2Cl chromophore. It emphasises the continuous transition from one structure to the next, with the directions of distortion determined by the modes of vibration, but with the observed structures determined by lattice packing factors.

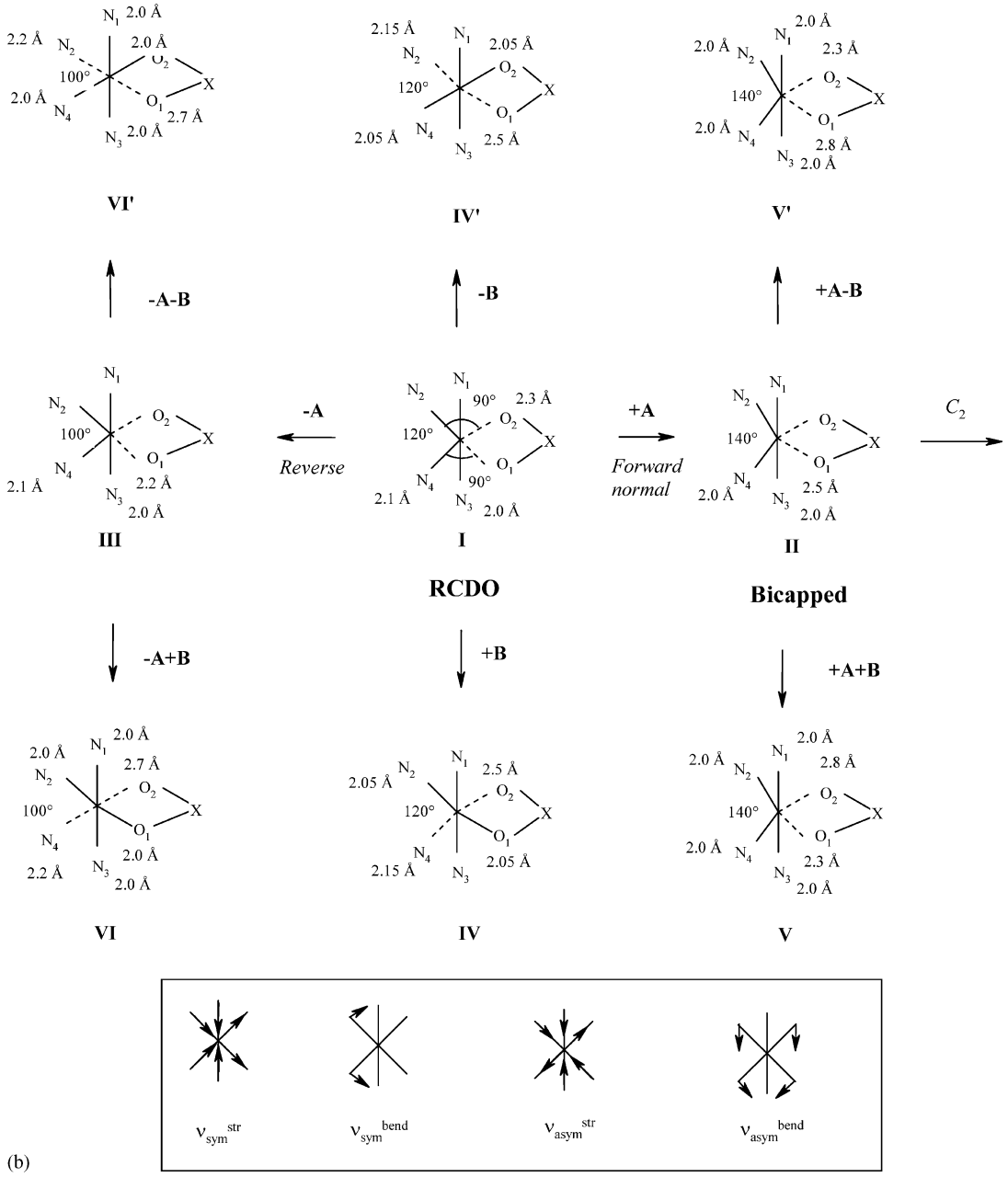

Fig. 9 (*Continued*)

6.2. Six coordinate systems

A comparable Structural Pathway may be drawn for the six coordinate *cis*-octahedral CuN_4X_2 chromophore, (CDO), but in practice this chromophore does not exist! It does occur in the CDO chromophore in the [Cu(chelate)$_2$(OXO)]Y series of complexes [13], where the $(OXO)^-$ anion is potentially a bidentate oxoanion (Fig. 9(b)). In order to retain similarity with Fig. 9(a), the $\pm$A$\pm$B route notation is retained in Fig. 9(b). In the CuN_4O_2 chromophore the highest symmetry of C_2 is retained along the central horizontal axis and controlled by the $\pm$A route distortion, *Forward normal* and *reverse*, as before, of the regular *cis*-distorted octahedral stereochemistry (RCDO). As the latter stereochemistry has not been characterised crystallographically to date, the dimensions of the central RCDO are only suggested values. The pure +A route distortions, ν_{sym}^{str} and ν_{sym}^{bend}, are characterised by an increase in the value of α_3 from ca. 120 to 140° and an increase in the Cu–O distances from 2.3 to 2.5 Å, at the extreme of which the stereochemistry is best referred to as a bicapped CuN_4O_2 chromophore intermediate between five and six coordination. This extreme stereochemistry with C_2 symmetry, has not been characterised either so far, but does occur coupled with the $\pm$B route distortion, ν_{asym}^{str}

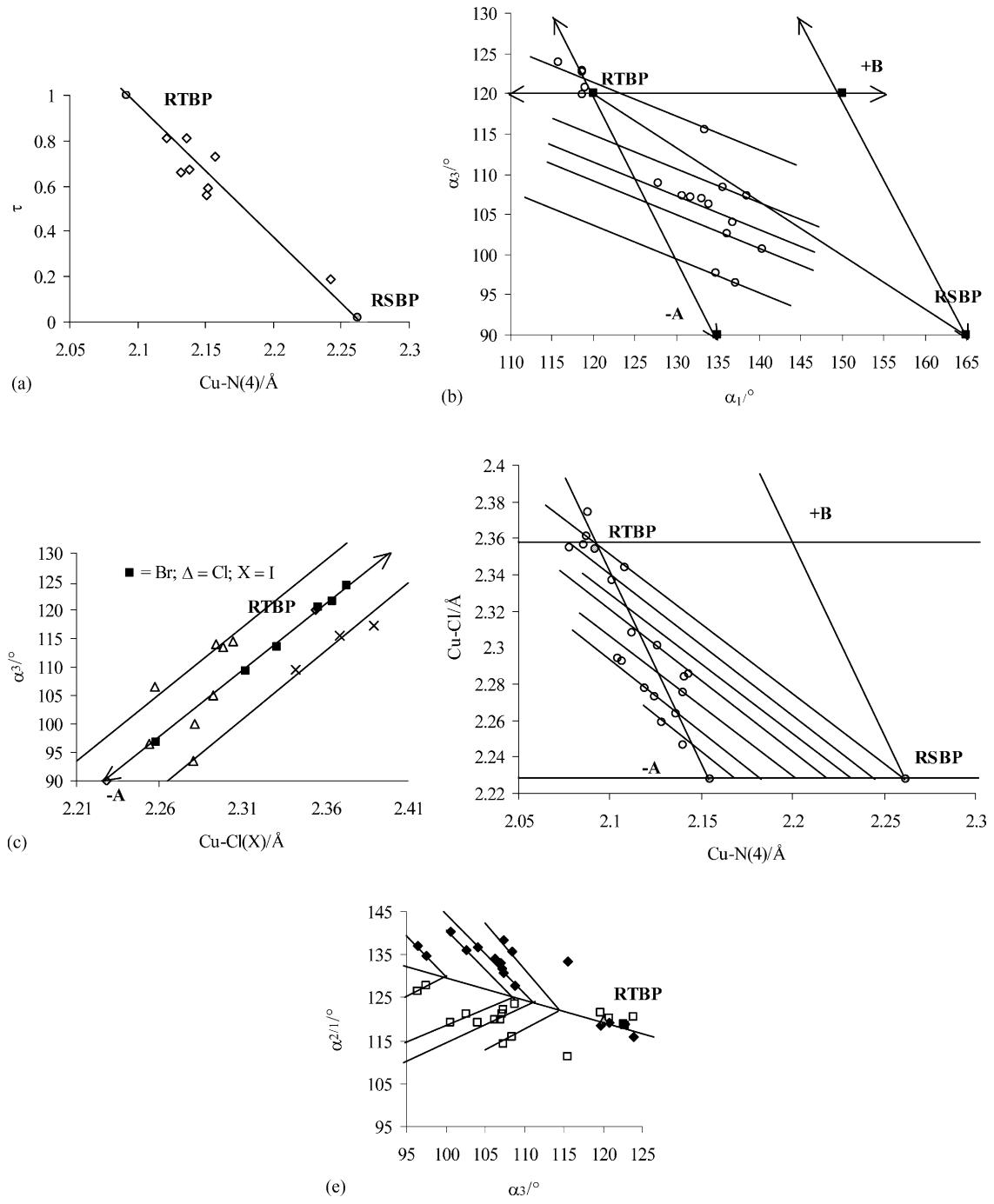

Fig. 10. (a) Plot of τ vs. Cu–N(4) for the $[Cu(phen)_2Cl][Y]$ series. (Ref. [75]. Copyright 1997. Reproduced by permission of The Royal Society of Chemistry.); (b) Plot of α_3 (ν^{bend}_{sym}) vs. α_1 (ν^{bend}_{asym}) for the $[Cu(bipy)_2Cl][Y]$ series. (Ref. [78]. Copyright 1999. Reproduced by permission of The Royal Society of Chemistry.); (c) Plot of α_3 (ν^{bend}_{sym}) vs. Cu–Cl(X) (ν^{str}_{sym}) for the $[Cu(phen)_2X][Y]$ series of complexes. (Ref. [75]. Copyright 1997. Reproduced by permission of The Royal Society of Chemistry.); (d) Plot of Cu–Cl (ν^{str}_{sym}) vs. Cu–N(4) (ν^{str}_{asym}) for the $[Cu(bipy)_2Cl][Y]$ series of complexes. (Ref. [78]. Copyright 1999. Reproduced by permission of The Royal Society of Chemistry.); (e) Plot of $\alpha_{2/1}$ vs. α_3 for the $[Cu(bipy)_2Cl][Y]$ series of complexes showing the formation of interpenetrating right-pointing arrowhead structures. (Ref. [78]. Copyright 1999. Reproduced by permission of The Royal Society of Chemistry.)

and ν^{bend}_{asym}, involving a net $+A\pm B$ route distortion, as seen in the complexes, $[Cu(phen)_2(O_2NO)][NO_3]$ [89] (**26**), $[Cu(MeTAAB)(O_2NO)][NO_3]\cdot H_2O$ [90] (**27**), and $[Cu(bipy)_2(O_2NO)][NO_3]\cdot H_2O$ [91] (**28**). The extent of the asymmetry of the Cu–O distances can be as high as 2.3–2.8 Å i.e. Δ 0.5 Å [91]. Although a pure $\pm B$ route distortion is theoretically possible for the RCDO stereochemistry, with $\alpha_3 = 120^\circ$, no crystal structures are known along this distortional route to date. A limited number of pure $-A$ route distorted CDO

stereochemistries are known, involving the $-\nu_{sym}^{str}$ and $-\nu_{sym}^{bend}$ modes, retaining the C_2 axis of symmetry with α_3 in the range 98–118°, respectively. However, these are a consequence of the PJTE, which are best referred to as *pseudo* CDO stereochemistries (Table 1), and should exhibit fluxional behaviour at sufficiently low temperatures. A typical example of such a complex is $[Cu(phen)_2(O_2CCH_3)][BF_4]\cdot 2H_2O$ [33,34] (**11**). Much more prolific are the $-A\pm B$ route distortions, with α_3 still in the range 98–118°, most which involve a static, highly asymmetric distorted structure, as observed in $[Cu(bipy)_2(ONO)][BF_4]$ [63] (**12**), $\Delta O = 0.35$ Å, but some are less distorted with near C_2 symmetry, as seen in $[Cu(bipy)_2(ONO)][NO_3]$ [13,35,86] (**33**), $\Delta O = 0.090(5)$ Å. These exhibit clear fluxional behaviour and must be considered as non-static *pseudo* CDO stereochemistries. The static asymmetric CDO stereochemistries can involve long Cu–O bond distances greater than 2.7 Å, generating a 4+1+1* coordination, which places these structures on the borderline between six and five coordination, again emphasising the idea of a continuous transition between the six coordinate RevCDO stereochemistry and the five coordinate SBP stereochemistry.

It is then significant that in the CDO Structural Pathway of Fig. 9(b), there is no extension of the $-A$ route distortion of the α_3 angles to lower values of 80–98°, as seen in the $[Cu(bipy)_2Cl]Y$ series [78], namely, into the see-saw range or as shown in 2000 by Palaniandavar et al., by the crystallographically reported novel structure, $[Cu(dipica)(NO_3)_2]$ [102] (**29**), which was reported with an α_3 as low as 80°, quite unique in copper(II) stereochemistry! Similarly, it is surprising to date, that there is no evidence of a short Cu–O bonded *cis*-octahedral CuN_4O_2 chromophore with Cu–O distances of 2.0 Å and an α_3 angle of ca. 90°, equivalent to the five coordinate see-saw stereochemistries observed for the six coordinate systems.

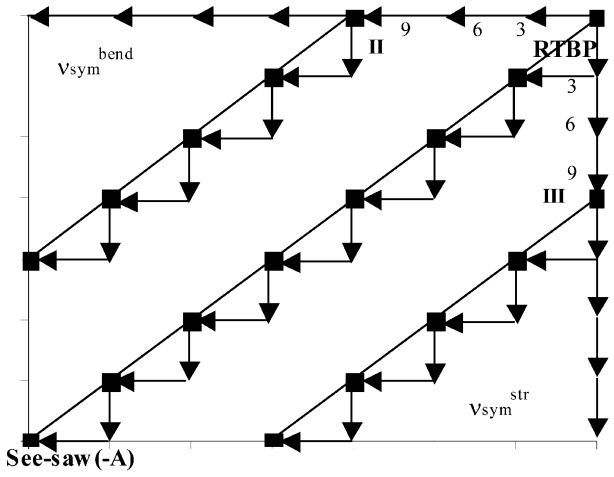

Fig. 11. Diagram illustrating how the linear and parallel pathways are formed by a progression of the coupled ν_{sym}^{str} and ν_{sym}^{bend} modes of vibration. (Ref. [75]. Copyright 1997. Reproduced by permission of The Royal Society of Chemistry.)

7. Evidence from scatter plot analysis for the continuous structural pathways in copper(II) stereochemistry

Crystallographic evidence for the existence of continuous structural pathways in copper(II) stereochemistries can be obtained from series of collective scatter plots of the copper–ligand bond distances and angles, obtained from a series of the same complex cation or anion. These may be from different forms of the same complex or from cation or anion distortion isomers of the same chromophore (e.g. the 18 cation distortion isomers of the $[Cu(bipy)_2Cl]^+$ cation) [78] as shown in the five examples of the scatter plots for the $[Cu(chelate)_2X]^+$ cation (Fig. 10(a)–(e)). Fig. 10(a), which is a plot of τ versus CuN(4) for the $[Cu(phen)_2Cl][Y]$ series [75], establishes that the data points are not randomly distributed about the RTBP and RSBP stereochemistries, but show a clear trend between the two, with some evidence for pathways parallel to the main trend line. In Fig. 10(b), which is a plot of α_3 versus α_1 for the $[Cu(bipy)_2Cl]Y$ series of complexes, a linear combination of the modes of vibration is again suggested [78]. Likewise, the parallel pathways of Fig. 10(c), which is a plot of α_3 (ν_{sym}^{bend}) versus Cu–Cl (ν_{sym}^{str}) for the $[Cu(phen)_2X][Y]$ series, suggest flips to parallel pathways implying horizontal and vertical progressions of the separate modes of vibration (Fig. 6). In order to explain the presence of parallel correlations in the scatter plots, n modes of a single vibration, $\pm\upsilon$, with $n = 8-10$, must be involved so that the parallel displacement can be seen, Fig. 11. This is then followed by progressive coupled modes, separate but parallel to the central correlation. The presence of both linear and parallel correlations in the same scatter plot has its roots in the amplification factor in the PJTE. This is one of the most convincing sources of evidence pointing to the presence of strutural pathways in such series of copper(II) complexes. In Fig. 10(d), which is a plot of Cu–Cl (ν_{sym}^{str}) versus Cu–N(4) (ν_{asym}^{str}) for the $[Cu(bipy)_2Cl][Y]$ series of complexes [78] the displacement of the Cu–N(4) distances to lower values can again be understood in terms of a horizontal flip through a progression of pure $n\nu_{asym}^{str}$ modes of vibration, giving a false association of the Cu–N(4) distances with the RTBP $-A$ route distortions. A feature of Fig. 10(e), which is a plot of $\alpha_{2/1}$ versus α_3 for the $[Cu(bipy)_2Cl][Y]$ series is the formation of interpenetrating right-pointing arrowhead structures, generated by the separate correlations of α_1 and α_2 data points against the α_3 angles. This suggests that as α_3 decreases there is a limit to the spread in $\Delta\alpha_{2,1}$, at which point the α_3 angle flips to a lower value, providing a clear graphical picture of the combi-

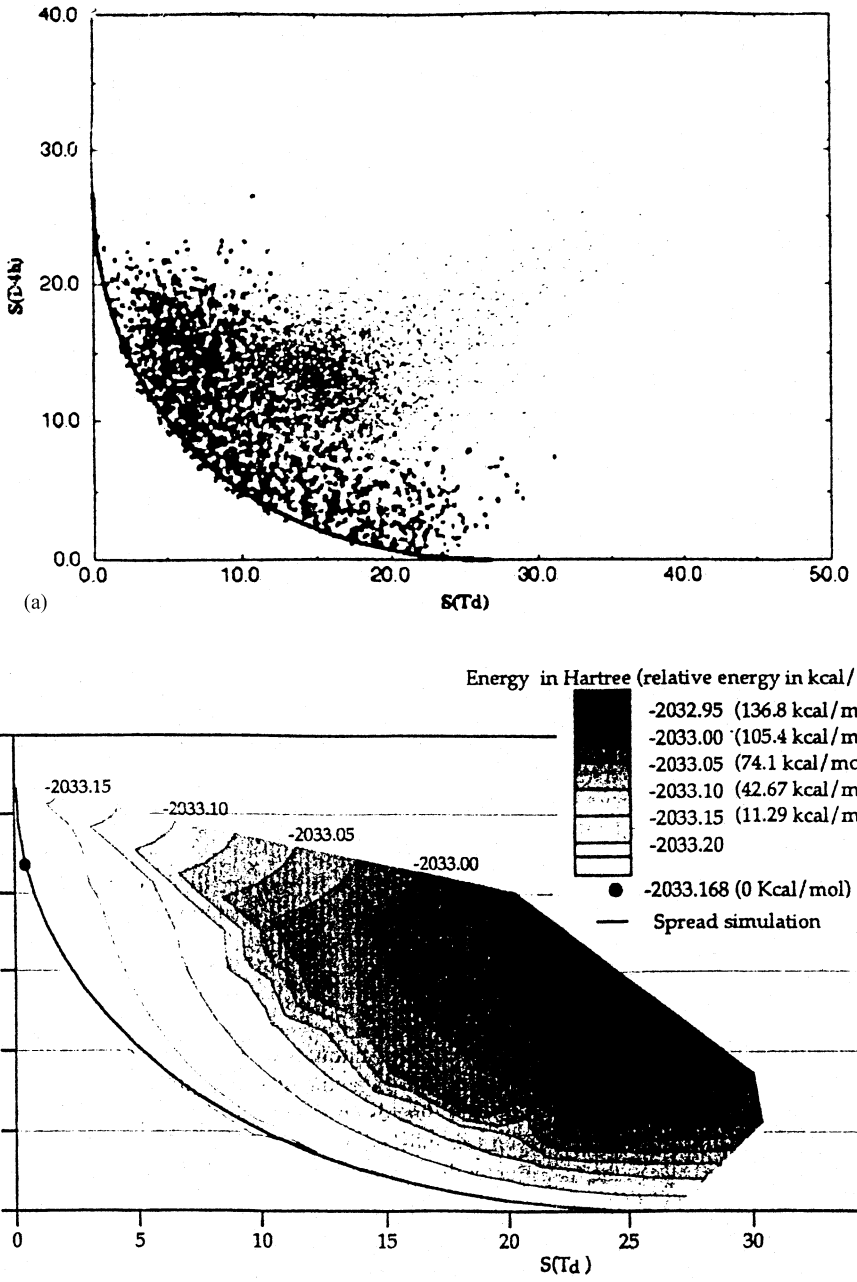

Fig. 12. (a) Degree of square planarity $S(D_{4h})$ vs. the degree of tetrahedricity $S(T_d)$ of 12,000 randomly created tetrahedral (all dots). A subgroup of 2000 random tetrahedral restricted by bond angles not smaller than 60° are shown also (black circles). Out of this cloud of possible tetracoordinated structures, copper complexes follow only the superimposed black line. (Reprinted with permission from Ref. [103]. Copyright 2001. American Chemical Society.); (b) Potential energy/symmetry surface of $CuCl_4^{2-}$. The spread is the black line. The global minimum is indicated by a black dot. (Reprinted with permission from Ref. [103]. Copyright 2001. American Chemical Society.)

nation of the ν_{sym}^{bend} and the ν_{asym}^{bend} modes of vibration (Fig. 11).

8. Continuous symmetry analysis

As outlined in previous work, attempts to correlate the physical properties of copper(II) complexes and their symmetry has received much attention by several authors in the literature [12,75–78,103,104]. One such example of this approach for the non-regular stereochemistries of the copper(II) ion has involved T, the tetragonality, given by the expression $T = R_S/R_L$, where R_S is the mean inplane (short bond length between the copper ligands) bond length and R_L is the mean out-of-the-plane (long bond length) bond length. T however is only applicable to the transition between the O_h and D_{4h} respective symmetries, generally with four long bond lengths and two shorter bond distances. The tetragonality itself is not constant, but is continuously variable

over certain limits. This implies that the eccentricity of the copper(II) ellipsoid is not fixed, so that the observed tetragonality can be determined by a number of minor effects, such as lattice packing forces, including van der Waals forces, hydrogen bonding and the nature of the non-equivalent ligands present. However, T must be considered as a *local* geometry measure. Another analogous local geometry measure parameter, used by Halvorson et al. [105] is θ, termed the *flattening* or *trans* angle of the four coordinate tetrahedral type complexes, which can vary from 109.5° for pure T_d symmetry to a maximum of 180° for SC D_{4h} symmetry. In using both such parameters, a specific direction of distortion from the ideal symmetry is assumed, meaning this approach is essentially local. In an interesting development in this context, a much more versatile tool, which has resulted in some recent pioneering publications in this area by a number of authors, is the use of CSM or continuous symmetry measure as a global descriptor, which incorporates simultaneously all variations in bond angles, bond distances, irrespective of their magnitude or direction [58,103,104]. CSM measures in a quantitative fashion the degree of symmetry within a given structure and the exact details of the algorithms, mathematical treatment and computational work underpinning this methodology can be found in several publications and references therein [106–108]. The CSM [103] can be defined as the minimum distance of a given structure to a complex having the desired symmetry, given by the expression:

$$S(G) = \min \frac{\sum_{k=1}^{N} |Q_k - \hat{P}_k|^2}{\sum_{k=1}^{N} |Q_k - Q_o|^2} \; 100$$

In this expression, if the distorted complex has N vertices (involving the central metal and associated ligands), with coordinates given by vectors $\bar{Q}_k$ ($k = 1, 2, 3, 4, \ldots, N$), a search is carried out to locate the coordinates of the vertex of the nearest perfectly symmetry object, given by the symmetry group, G. These coordinates can be described by the vectors $\bar{P}_k$ ($k = 1, 2, 3, 4, \ldots, N$). The distance of the complex then to the perfect polyhedron belonging to this G symmetry group is given by the $S(G)$ expression above. In this equation, Q_o is defined as the coordinate vector of the centre of mass of the complex under examination.

Keinan and Anvir have explored [103] the symmetry of tetracoordinated copper(II) complexes, including the four coordinate $[CuCl_4]^{2-}$ and $[CuBr_4]^{2-}$ series using this approach of quantitative continuous symmetry. They found extraordinarily, in 2001, that of the vast database of geometry allowed complexes, spanning the $S(T_d)$ (tetrahedral) and $S(D_{4h})$ (SC) pair values, all the copper(II) structures fall incredibly into a very well defined correlation line, linking the two symmetry-content measures. The more general $S(D_{4h})$ versus $S(T_d)$ plot however, as shown in Fig. 12, consisting of ca. 12,000 tetrahedra, using the Cambridge Crystallographic Database (CSD), yielded a much broader and dispersed pattern. As commented by the authors, it is remarkable when examining such a strongly defined correlation line evident in this overall cluster plot, to observe the result of the various forces of distortion, including JT effects, crystal packing, intramolecular forces, protein folding etc. all funnelled to the same coordinates of $S(D_{4h})/S(T_d)$ line, and not scattered over the general region of possible structures in Fig. 12(a). In order to explore further the nature of the distortion from T_d to D_{4h} symmetry, Keinan and Anvir examined the three tetrahedral planarisation modes, namely the twist, compression and spread routes of distortion of four coordinate species and found the dominance of the B_{2u} or spread mode of vibration, in particular in the $[CuCl_4]^{2-}$ series, although an equally good fit was found in other series also. On calculating the PES they found that the minimal molecular symmetry distortive spread correlation line coincided with the sole energy valley of the map (Fig. 12(b)).

In a related paper in the same year (2001) [104], Keinan and Anvir also looked at correlations between symmetry and d–d electronic transitions, ESR $g_{\|}$ and structural responses to variations in temperature, in particular for four- and six coordinate copper(II) complexes, including the blue copper proteins (BCPs). In the case of the temperature effects on symmetry, they quoted two interesting examples. In the $[CuCl_6]^{2-}$ anion in $[3\text{-}ClC_6H_4NH_3]_8CuCl_{10}$ (**61**), it was found that the degree of octahedricity, $S(O_h)$, increased with temperature over a range 156–295 K, respectively. In direct contrast, in the CuN_6 chromophore in $[Cu(mtz)_6]^{2+}$ (**62**), an opposite effect was found. The complex itself consists of two crystallographically non-equivalent molecules in the unit cell. In the first stereochemistry, A, the CuN_6 chromophore, using ESR measurements, was suggested to belong to one of the three potential energy wells of the *Mexican Hat* warped energy surface as mentioned earlier in this review. In the second case, A′, the incorporation of all three energy wells was proposed based on the density of scattering. As the temperature increased, $S(O_h)$ was found to decrease in both sites A and A′, respectively, but initiated at a much higher value in the case of A (close to 0.65), indicative of an enhanced degree of distortion, unlike A″ which started at ca. 0.12. At high temperature, 295 K, $S(O_h)$ for A had fallen from ca. 0.65 to 0.4, whereas for A′, the corresponding plummet of degree of distortion, was from ca. 0.12 to 0.05. Keinan and Anvir rationalised this rather unique phenomenon in terms of a surge in the rate of hopping between the energy wells with increasing temperature. At low values of temperature, the lowest energy minimum is mainly the most populated one. However, at higher values of temperature, the dynamic JTE is not in

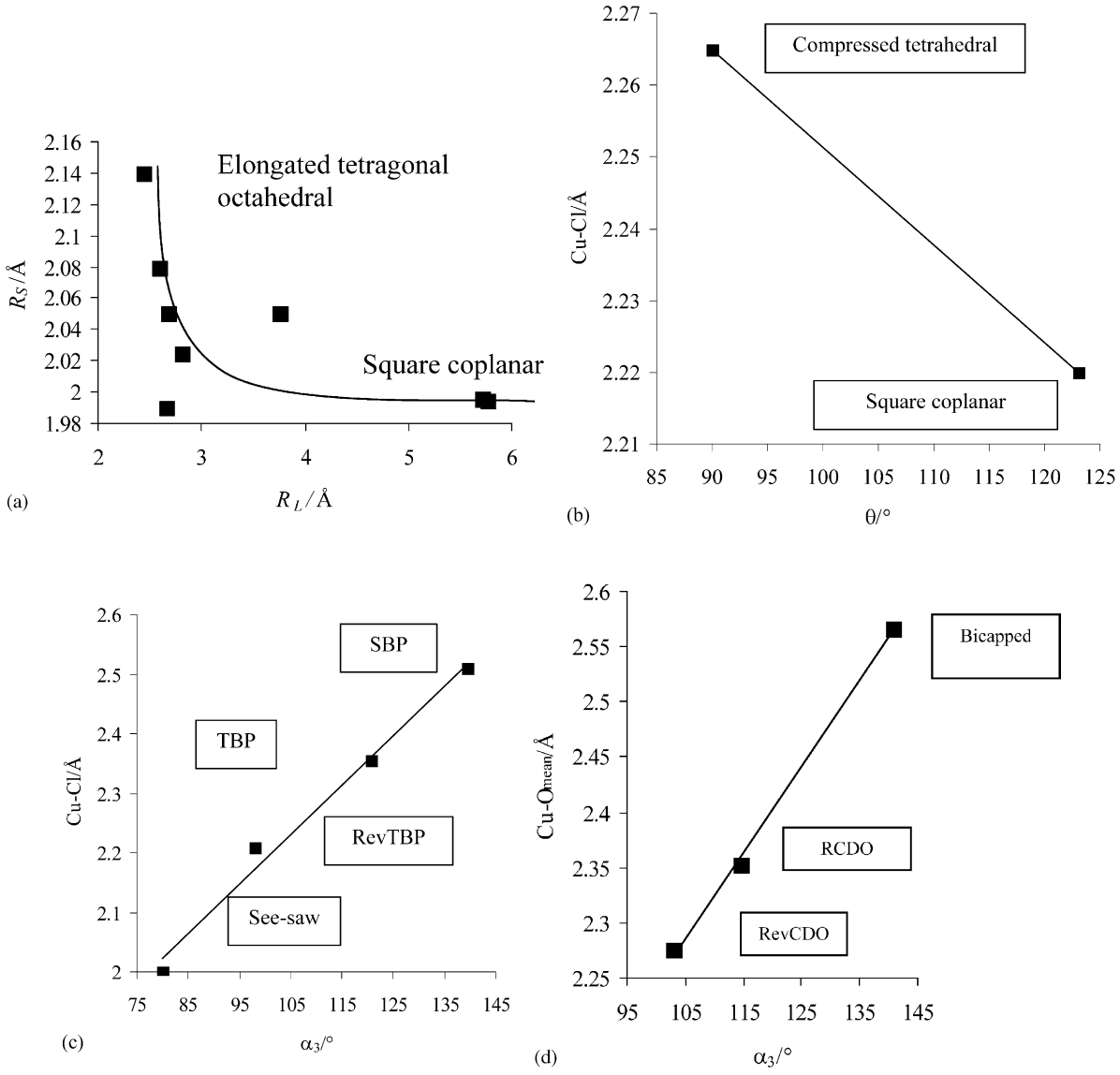

Fig. 13. (a) Plot of R_S vs. R_L for the $[Cu(NH_3)_2X_2]$ series [54,67] from SC, T ($=R_S/R_L$) = 0.34 (SC) to elongated tetragonal tetrahedral (ETO), T = 0.88. (b) Plot of Cu–Cl vs. θ for the $[CuCl_4]^{2-}$ series [61] from CT to SC. (c) Plot of Cu–Cl vs. α_3 for five coordinate complexes from see-saw to RevTBP, to TBP, to SBP. Selected examples of such complexes are: See-saw: $[Cu(dipica)(NO_3)_2]$ [102] (**29**), (2.000 Å, 80°); RevTBP: $[Cu(terpyBr_2]$ [114] (**30**), (2.353 Å, 109°) TBP: $[Cu(bipy)_2Cl]/2OH \cdot 1/2Cl^{1/3}$ (**32**), (2.354 Å, 120.7°); SBP: $[Cu(phen)_2(OH_2)][NO_3]$ [62] (**34**), (2.51 Å, 139.6°). (d) Plot of Cu–O_{mean} vs. α_3 for six coordinate complexes going from RevCDO to RCDO, to bicapped square pyramidal stereochemistries.

operation and thermal population of the higher energy minima takes place. The net effect of this process is that the various populations begin to equalise each other, resulting in an averaging of the various types of distortion, into a much less distorted stereochemistry. In the case of the $[Cu(mtz)_6]^{2+}$ moiety (**62**), sufficient volume is present for expansion at higher temperature values. This is not the situation in the $[CuCl_6]^{2-}$ anion in $[3\text{-}ClC_6H_4NH_3]_8CuCl_{10}$ (**61**).

In the case of five coordinate copper(II) complexes, Alvarez and Llunell in 2000, have also used the CSM approach to explore the Berry and non-Berry distortions of the RTB stereochemistry [58]. These authors have described at length the angular distortions involving the Berry *pseudo* rotation pathway and the SBP stereochemistry and non-Berry angular distortions including the Reverse Berry distortion and Umbrella distortions. They found that the Berry *pseudo* rotation pathway is well described by both the angular parameter, τ, and S (TBP). However, they did find that although CSM can discriminate between different SP structures, τ, presents the same value for any C_{4v} SP system. In this work, they found that if bi- and tridentate ligands are involved, the large gamut of complexes of the $[Cu(bipy/phen)_2X]^+$ and $[M(terpy)X_2]$ series [78] are not adequate models to describe the Berry *pseudo* rotation pathways.

In earlier work, 1997, Bukowska-Stryzewska et al. analysed 154 dinuclear di-μ-chloro, bromo and fluoro

five coordinate (4+1) copper complexes using structure correlation methods, again showing the power of comparative X-ray crystallography in this area of research [109]. In related developments, correlations between energy and symmetry have been shown in the enantiomerizations of chiral fullerenes [110] and even more recently in the binding of HIV C_2 inhibitors [111], an area of research, which has huge global ramifications, particularly in medicine.

9. Some conclusions and implications of the presence of continuous structural pathways in copper(II) stereochemistry

Taken together, structural pathways suggest that the structures of the individual copper(II) complexes are related by the modes of vibration of the in-plane CuN_2X_n chromophore, with each structure representing a stable structure in the vibronic potential energy well on the PES of the respective cation, with the separate structures determined by crystal packing factors i.e. hydrogen bonding and van der Waal forces. As these are relatively small, less than 10 kcals mol^{-1}, it is not surprising that the energy barrier between the separate wells is not of a significantly high value and accounts for the almost continuous range in stereochemistry observed for a given cation distortion isomer, as exemplified in the $[Cu(bipy)_2Cl][Y]$ series [78].

It can now be seen that structural pathways play a pivotal role in the interpretation of copper(II) stereochemistry (Fig. 13(a)–(d)). In the wider context of copper(II) stereochemistry the simple static picture is no longer realistic, as the role of vibronic coupling is increasingly better understood in creating continuous structural pathways between these extreme stereochemistries. Nevertheless, it is important to remember that the actual stereochemistry of a complex is determined by relatively weak packing forces culminating in a number of practical implications, some of which are obvious:

a) Recrystallisation of a given complex or cation distortion isomer under different conditions of temperature or pressure or from a different solvent may result in significantly different structural results, even in the same space group [112]. Such differences may result in the spectroscopic results being slightly different if the complex has been prepared under different conditions from those used in the original preparation, even if these are measured in the solid state. It is not advised to compare solution spectra with that measured in the solid state, for the same reason.
b) The use of a series of cation distortion isomers to see how the cation environment varies with the anion present, although rudimentary, is seen as an effective way, of varying the crystal environment of the cation [113].
c) The past practice of preparing a series of [Cu(ligand)X] type complexes, determining the structure of one complex and assuming that the structure of the whole series is the same, is clearly no longer justified unless a close examination of the spectroscopic properties justify this assumption.
d) The extensive time spent on examining the properties of the fluxional or temperature variable properties of high symmetry copper(II) complexes is now seen to have been of less importance in terms of describing the structures of static copper(II) complexes. However, these fluxional systems were important in establishing the role of vibronic coupling that can now be used to account for the continuous variability of the copper(II) stereochemistries that is portrayed in the graphical picture of structural pathways.

Acknowledgements

The authors would like to acknowledge the pioneering work of many of the individual researchers and their respective co-workers, whose comprehensive work and in-depth accounts have been referenced extensively in this review, and whose own individual reviews in the area of JT has contributed enormously to our knowledge in this field, in particular in our own niche of vibronic coupling and structural pathways. In particular, the authors acknowledge I.B. Bersuker, The University of Texas at Austin, L. Falvello, University of Zarago, C.J. Simmons, University of Hawaii at Hilo, M. Hitchman, University of Tasmania, S. Alvarez, Universitat de Barcelona, S. Keinan and D. Avnir, The Hebrew University of Jerusalem and H. Bürgi, University of Bern for their own profound reviews in this field, covering many of the facets and perspectives referred to in this paper. In addition, M.B. Hursthouse and the chemical crystallography research group at the EPSRC National Crystallography Service, University of Southampton, UK, are thanked for their continued and loyal support in the provision of state-of-the-art crystallographic facilities for pursuing this new emerging field in structure systematics of comparative X-ray crystallography. The United Arab Emirates University Research Council, are also acknowledged for funding individual projects (01/11-2-03 and 02/10-2-11), under the Limited Research Grant Schemes for the years 2001 and 2002 in continued research in this growing area of copper(II) stereochemistry involving structure correlation analysis.

References

[1] H.A. Jahn, E. Teller, Proc. R. Soc. 161 (1937) 220.
[2] I.B. Bersuker, Chem. Rev. 101 (2001) 1067.
[3] R. Engleman, B. Halperin, M. Weger, Physica C 169 (1990) 314.
[4] S. Jin, T.H. Tiefel, M. McCormack, R.A. Fastnacht, R. Ramesh, L.H. Chen, Science 264 (1994) 413.
[5] Yu.B. Gaididei, V.M. Loktev, Phys. Status Solidi 147 (1988) 307.
[6] W. Weber, A.L. Shelankov, X. Zotos, Physica C 162-164 (1989) 307.
[7] D.V. Fil, O.I. Tokar, A.L. Shelankov, W. Weber, Phys. Rev. B 45 (1992) 5633.
[8] H. Koizumi, I.B. Bersuker, Phys. Rev. Lett 83 (1999) 3009.
[9] J.L. Dunn, M.R. Eccles, Phys. Rev. B 64 (2001) 195104.
[10] B.J. Hathaway, M. Duggan, A. Murphy, J. Mullane, C. Power, A. Walsh, B. Walsh, Coord. Chem. Rev. 36 (1981) 267.
[11] B.J. Hathaway, Coord. Chem. Rev. 35 (1981) 211.
[12] B.J. Hathaway, Struct. Bonding (Berlin) 57 (1984) 56.
[13] C.J. Simmons, New. J. Chem. 17 (1993) 77.
[14] I.B. Bersuker, Coord. Chem. Rev. 14 (1975) 357.
[15] M.A. Hitchman, Comments Inorg. Chem. 15 (1994) 197.
[16] L. Falvello, J. Chem. Soc. Dalton Trans. (1997) 4463.
[17] I.B. Bersuker, Electronic Structure and Properties of Transition Metal Compounds. Introduction to the Theory, Wiley, New York, 1996.
[18] C.J. Simmons, Struct. Chem. 3 (1992) 25.
[19] G.S. Beddard, M.A. Halcrow, M.A. Hitchman, M.P. de Miranda, C.J. Simmons, H. Stratemeier, Dalton Trans. 5 (2003) 1028.
[20] M. Gerloch, Inorg. Chem. 20 (1981) 638.
[21] R.J. Deeth, M.A. Hitchman, Inorg. Chem. 25 (1986) 1225.
[22] G. Wingefeld, R. Hoppe, Z. Anorg. Allg. Chem. 516 (1984) 223.
[23] B.J. Hathaway, D.E. Billing, Coord. Chem. Rev. 5 (1970) 143.
[24] A.C. Blackburn, J.C. Gallucci, R.E. Gerkin, Acta Crystallogr. Sect. C 47 (1991) 2019.
[25] J.H. Ammeter, H.B. Bürgi, E. Gamp, V. Meyer-Sandrin, W.P. Jensen, Inorg. Chem. 18 (1979) 733.
[26] D. Mullen, G. Heger, D. Reinen, Solid State Commun. 17 (1975) 1249.
[27] N.W. Alcock, M. Duggan, A. Murray, S. Tyagi, B.J. Hathaway, A. Hewat, J. Chem. Soc. Dalton Trans. (1984) 7.
[28] R.S. Markiewicz, J. Phys. Chem. Solids 15 (1995) 1637.
[29] M. Bacci, New J. Chem. 17 (1993) 67.
[30] M.J. Riley, M.A. Hitchman, D. Reinen, Chem. Phys. 102 (1986) 11.
[31] D. Reinen, S. Krause, Inorg. Chem. 20 (1981) 2750.
[32] C. Friebel, V. Propach, D. Reinen, Z. Naturforsch. 31B (1976) 1574.
[33] F. Clifford, E. Counihan, W. Fitzgerald, K. Seff, C.J. Simmons, S. Tyagi, B.J. Hathaway, J. Chem. Soc. Chem. Commun. (1982) 196.
[34] C.J. Simmons, K. Seff, F. Clifford, B.J. Hathaway, Acta. Crystallogr. C39 (1983) 1360.
[35] C.J. Simmons, B.J. Hathaway, K. Amornjarusiri, B.D. Santarsiero, A. Clearfield, J. Am. Chem. Soc. 109 (1987) 1947.
[36] M.J. Riley, M.A. Hitchman, D. Reinen, G. Steffen, Inorg. Chem. 27 (1988) 1924.
[37] P. Chaudhuri, K. Oder, K. Wieghardt, J. Weiss, J. Reedijk, W. Hinricks, J. Wood, A. Ozarowski, H. Stratemeier, D. Reinen, Inorg. Chem. 25 (1986) 2951.
[38] I.B. Bersuker, The Jahn–Teller Effect and Vibronic Interactions in Modern Chemistry, Plenum, New York, 1984.
[39] D. Reinen, M. Atansov, Magn. Reson. Rev. 15 (1991) 167.
[40] W.J.A. Maaskant, Struct. Bonding (Berlin) 83 (1995) 55.
[41] T. Ogihara, J. Phys. Soc. Jpn. 64 (1995) 4221.
[42] M.A. Hitchman, W. Maaskant, J. van der Plas, C.J. Simmons, H. Stratemeier, J. Am. Chem. Soc. 121 (1999) 1488.
[43] A.J. Schultz, M.A. Hitchman, J.D. Jörgensen, S. Lukin, P.G. Radelli, C.J. Simmons, H. Stratemeier, Inorg. Chem. 36 (1997) 3382.
[44] B.N. Figgis, B.B. Iversen, F.K. Larsen, P.A. Reynolds, Acta Crystallogr. B49 (1993) 794.
[45] C.J. Simmons, M.A. Hitchman, H. Stratemeier, A.J. Schultz, J. Am. Chem. Soc. 115 (1993) 11304.
[46] C.J. Simmons, M.A. Hitchman, H. Stratemeier, T. Astley, Inorg. Chem. 39 (2000) 4651.
[47] R. Jakobi, H. Spiering, E. Gmelin, P. Gütlich, Inorg. Chem. 27 (1988) 1823.
[48] M.A. Augustyniak-Jablokow, Yu.V. Yablokov, K. Lukaszewicz, A. Pietraszko, V.E. Petrashen, V.A. Ulanov, Chem. Phys. Lett. 344 (2001) 345.
[49] B.J. Hathaway, D.E. Billing, Coord. Chem. Rev. 5 (1970) 143.
[50] J.T. Hougen, G.E. Lenoi, T.C. James, J. Chem. Phys. 34 (1961) 1670.
[51] I. Bernal, J.D. Korp, E.O. Schlemper, M.S. Hussain, Polyhedron 1 (1982) 365.
[52] N. Ray, L. Hulett, R. Sheahan, B.J. Hathaway, J. Chem. Soc. Dalton Trans. (1981) 1463.
[53] M. Duggan, N. Ray, B.J. Hathaway, G. Tomlinson, P. Brint, K. Pelin, J. Chem. Soc. Dalton Trans. (1980) 1342.
[54] F. Hanic, Acta Crystallogr. 12 (1959) 739.
[55] C. Friebel, Z. Anorg. Allg. Chem. 417 (1975) 197.
[56] R.V.G. Sundara Rao, K. Sundaramma, G. Sivasankard Rao, Z. Kristallogr. 110 (1958) 231.
[57] (a) D.L. Cullen, E.C. Lingafelter, Inorg. Chem. 10 (1971) 1264; (b) D. Reinen, C. Friebel, Struct. Bonding (Berlin) 37 (1979) 1.
[58] S. Alvarez, M. Llunell, J. Chem. Soc. Dalton Trans. (2000) 3288.
[59] S. Takagi, P.G. Lenhert, M.D. Jöesten, J. Am. Chem. Soc. 96 (1974) 6606.
[60] A. Pabst, Acta Crystallogr. 12 (1959) 733.
[61] (a) L. Helmholtz, R.F. Kruh, J. Am. Chem. Soc. 74 (1952) 1176; (b) J.A. McGinnety, J. Am. Chem. Soc. 94 (1972) 8406.
[62] H. Nakai, Y. Noda, Bull. Chem. Soc. Jpn. 51 (1978) 1386.
[63] A. Walsh, B. Walsh, B. Murphy, B.J. Hathaway, Acta Crystallogr. Sect. B 37 (1981) 1512.
[64] A.F. Cameron, D.W. Taylor, R.H. Nuttall, J. Chem. Soc. Dalton Trans. (1972) 1603.
[65] D.A. Langs, C.R. Hare, J. Chem. Soc. Chem. Commun. (1967) 890.
[66] J. Gazo, I.B. Bersuker, J. Garaj, M. Kabesova, J. Kohout, H. Langfelderova, M. Melnik, M. Serator, F. Valach, Coord. Chem. Rev. 19 (1976) 253.
[67] J.A. Cahajdova, F. Hanic, Acta Crystallogr. 11 (1958) 610.
[68] A. Pajunen, K. Smolander, I. Belinskij, Suom. Kemistilehti. Sect. B 45 (1972) 317.
[69] S. Takagi, M.D. Jöesten, P.G. Lenhert, Acta Crystallogr. Sect. B 32 (1976) 1278.
[70] W.D. Harrison, D.M. Kennedy, N.J. Ray, R. Sheahan, B.J. Hathaway, J. Chem. Soc. Dalton Trans. (1981) 1556.
[71] S.G. Teoh, H.K. Fun, B.T. Chan, J. Fizik Mal. 8 (1987) 44.
[72] J. Foley, S. Tyagai, B.J. Hathaway, J. Chem. Soc. Dalton Trans. (1990) 3399.
[73] P. Nagle, E. O'Sullivan, B.J. Hathaway, E. Muller, J. Chem. Soc. Dalton Trans. (1990) 3399.
[74] H. Bürgi, J.D. Dunitz, Acc. Chem. Res. 16 (1983) 153.
[75] G. Murphy, P. Nagle, B. Murphy, B. Hathaway, J. Chem. Soc. Dalton Trans. (1997) 2645.
[76] G. Murphy, C. Murphy, B. Murphy, B. Hathaway, J. Chem. Soc. Dalton Trans. (1997) 2653.
[77] G. Murphy, C. O'Sullivan, B. Murphy, B. Hathaway, Inorg. Chem. 37 (1998) 240.

[78] C. O'Sullivan, G. Murphy, B. Murphy, B. Hathaway, J. Chem. Soc. Dalton Trans. (1999) 1835.
[79] K.G. Shields, C.H.L. Kennard, Cryst. Struct. Commun. 1 (1972) 189.
[80] H. Montgomery, E.C. Lingalfelter, Acta Crystallogr. 20 (1966) 659.
[81] M. Bukovska, M.A. Porai-Koshits, Zh. Strukt. Khim. 7 (1961) 712.
[82] (a) A. Ferrari, A. Bribanti, T. Tiripicchio, Acta Crystallogr. 21 (1966) 605;
(b) B.J. Hathaway, F.S. Stephens, J. Chem. Soc. (A) (1970) 884.
[83] D.S. Brown, J.D. Lee, B.G.A. Melson, Acta Crystallogr. Sect. B 24 (1968) 730.
[84] (a) G. Giuseppetti, F. Mazzi, Rend. Soc. Min. Ital. 11 (1955) 202;
(b) R.D. Ball, D. Hall, C.E.F. Rickard, T.N. Waters, J. Chem. Soc. (A) (1967) 1435.
[85] M. Brophy, G. Murphy, C. O'Sullivan, B.J. Hathaway, B. Murphy, Polyhedron 18 (1999) 611.
[86] I.M. Procter, F.S. Stephens, J. Chem. Soc. (A) (1969) 1248.
[87] B. Murphy, Ph.D. Thesis, National University of Ireland, 1994.
[88] B. Murphy, M. Aljabri, M. Light, M.B. Hursthouse, J. Chem. Crystallogr 33 (3) (2003) 195.
[89] K. Amornjarusiri, Ph.D. Thesis, National University of Ireland, 1986.
[90] A.J. Jirocitano, R.I. Sheldon, K.B. Mertes, J. Am. Chem. Soc. 105 (1983) 3022.
[91] (a) R.J. Fereday, P. Hodgson, S. Tyagi, B.J. Hathaway, J. Chem. Soc. Dalton Trans. (1981) 2070;
(b) R.J. Fereday, P. Hodgson, S. Tyagi, B.J. Hathaway, Inorg. Nucl. Chem. Lett. 17 (1981) 243.
[92] S.J. Hill, P. Hubberstey, W.-S. Li, Polyhedron 16 (1997) 2447.
[93] H.B. Bürgi, Acta Crystallogr. A54 (1998) 873.
[94] R. Hoffmann, Am. Sci. 86 (1997) 15.
[95] H.B. Bürgi, J.D. Dunitz, Structure Correlation, VCH, Weinheim, 1993.
[96] T. Auf der Heyde, Angew. Chem. Int. Ed. Engl. 33 (1994) 823.
[97] H.B. Bürgi, J.D. Dunitz, J. Am. Chem. Soc. 97 (1975) 921.
[98] H.B. Bürgi, Inorg. Chem. 12 (1973) 2321.
[99] F.W.B. Einstein, A.C. MacGregor, J. Chem. Soc. Dalton Trans. (1974) 778.
[100] D.R. Storm, D.E. Koshland, J. Am. Chem. Soc. 94 (1972) 5805.
[101] R.R. Holmes, Pentacoordinated Phosphorus. Am. Chem. Soc. Monogr. No. 175/176, American Chemical Society, Washington, DC, 1980.
[102] M. Palaniandavar, S. Mahadevan, M. Köckerling, G. Henkel, J. Chem. Soc. Dalton Trans. (2000) 1151.
[103] S. Keinan, D. Anvir, Inorg. Chem. 40 (2001) 318.
[104] S. Keinan, D. Anvir, J. Chem. Soc. Dalton Trans. (2001) 941.
[105] K.E. Halvorson, C. Patterson, R.D. Willett, Acta Crystallogr. B46 (1990) 508.
[106] H. Zabrodsky, S. Peleg, D. Avnir, J. Am. Chem. Soc. 114 (1992) 7843.
[107] H. Zabrodsky, S. Peleg, D. Avnir, J. Am. Chem. Soc. 117 (1995) 462.
[108] Y. Salomon, D. Avnir, J. Comput. Chem. 20 (1999) 772.
[109] M. Bukowska-Stryżewska, W. Maniukiewicz, L. Sieroń, Acta Cryatallogr. B53 (1997) 466.
[110] Y. Pinto, P.W. Fowler, D. Mitchell, D. Anvir, J. Phys. Chem. B 102 (1998) 5776.
[111] S. Keinan, D. Anvir, J. Am. Chem. Soc. 122 (2000) 4378.
[112] G. Roberts, Ph.D. Thesis, National University of Ireland, 1998.
[113] D. Cunningham, Ph.D. Thesis, National University of Ireland, 1992.
[114] M.J. Arriorta, J.L. Mesa, T. Rojo, T. Debaerdemaeker, D. Beltran-Porter, H. Stratemeir, D. Reinen, Inorg. Chem. 27 (1988) 2976.